Shortening of continental lithosphere: the neotectonics of Eastern Anatolia — a young collision zone

J.F. Dewey, M.R. Hempton, W.S.F. Kidd, F. Saroglu & A.M.C. Şengör

SUMMARY: We use the tectonics of Eastern Anatolia to exemplify many of the different aspects of collision tectonics, namely the formation of plateaux, thrust belts, foreland flexures, widespread foreland/hinterland deformation zones and orogenic collapse/distension zones. Eastern Anatolia is a 2 km high plateau bounded to the S by the southward-verging Bitlis Thrust Zone and to the N by the Pontide/Minor Caucasus Zone. It has developed as the surface expression of a zone of progressively thickening crust beginning about 12 Ma in the medial Miocene and has resulted from the squeezing and shortening of Eastern Anatolia between the Arabian and European Plates following the Serravallian demise of the last oceanic or quasi-oceanic tract between Arabia and Eurasia. Thickening of the crust to about 52 km has been accompanied by major strike-slip faulting on the right-lateral N Anatolian Transform Fault (NATF) and the left-lateral E Anatolian Transform Fault (EATF) which approximately bound an Anatolian Wedge that is being driven westwards to override the oceanic lithosphere of the Mediterranean along subduction zones from Cephalonia to Crete, and Rhodes to Cyprus. This neotectonic regime began about 12 Ma in Late Serravallian times with uplift from widespread littoral/neritic marine conditions to open seasonal wooded savanna with colluvial, fluvial and limnic environments, and the deposition of the thick Tortonian Kythrean Flysch in the Eastern Mediterranean. Earthquake hypocentres are scattered throughout the region but large earthquakes are concentrated mainly on the major faults and are mostly shallow, supporting the idea of a brittle elastic lid with hypocentres concentrated towards its base with more ductile deformation in the middle and lower crust. Neotectonic magmatic suites are nepheline-hypersthene normative alkali basalts of mantle origin, and silicic/intermediate/mafic calc-alkaline suites, both suites occurring in pull-apart basins in strike-slip regimes and along N–S extensional fissures, and both suites showing a strong change to central activity in the Pliocene. Upper-crustal strains appear to be discontinuous in space and time, with zones of strong shortening representing shoaling of crustal detachment zones flattening between 5 and 10 km. Approximately NW- (dextral) and NE- (sinistral) trending lineaments bound less deformed wedges (low relief seismically 'dead' areas) and vary from simple strike-slip faults to complicated braided transform–flake boundaries with pull-apart and compressional segments (N and E Anatolian Transform Faults). Volcanoes lie in grabens on N–S 'cracks' that extend into the Arabian Foreland and in transcurrent pull-aparts. Major extensional basins lie at plate (Adana) and flake (Karliova) triple junctions and result from compatibility problems.

Apart from impacts and possible but difficult to evaluate sub-lithospheric influences, the geology of the continental crust is the consequence of the flexure, stretching and shortening of the lithosphere. Rapid stretching and shortening of the lithosphere produce isothermal thinning and thickening respectively, with consequent basins and mountains. Thermal relaxation generates further subsidence or uplift, enhanced, respectively, by sedimentation and denudation. Consequently, most vertical motions leading to all the subtleties and complexities of stratigraphic development are the result of lithospheric deformation. Continental collision is one of the principal mechanisms leading to lithospheric/crustal thickening and mountain building and is an appropriate topic for a William Smith thematic meeting honouring Robert Shackleton, that prime observer and interpreter of rocks in continental deformation zones.

Continental collision involves the progressive impingement of buoyant or highstanding terranes with subduction zones. All scales and variations exist on this theme between the collision of seamounts and seamount chains with arcs through the collision of oceanic plateaux and microcontinents with arcs to the collision of large continental masses. The scale of collision dictates the style, duration and intensity of the resulting strain systems and sequences (Dewey 1977). Colliding continental margins are irregular and strain sequences are usually diachronous along great strike lengths along suture zones (Dewey & Burke 1973). Prior to terminal continental collision, one or both continental margins may have had a long and complex history of exotic terrane assembly (Coney *et al.*, 1980).

Continental convergent plate boundaries such as the Alpine/Himalayan System (Fig. 1), are wide, diffuse and complicated zones where relative plate displacements are converted into

From COWARD, M. P. & RIES, A. C. (eds), 1986, *Collision Tectonics*, Geological Society Special Publication No. 19, pp. 3–36.

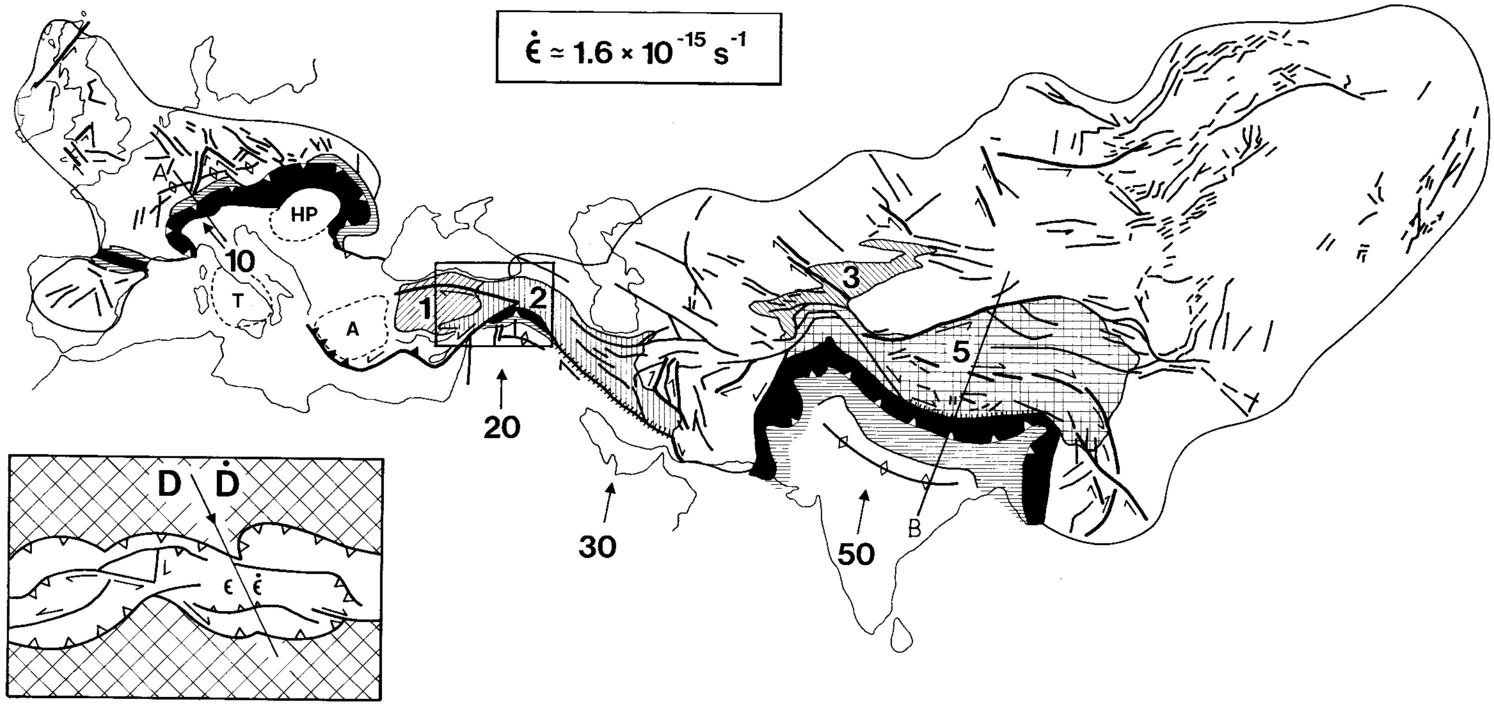

FIG. 1. Simplified tectonic map of the Alpine/Himalayan convergent system. Plate slip rates (Minster *et al.* 1974) in mm yr^{-1} in the Eurasian reference frame. Thrust belts: black; foreland and hinterland basins: horizontal lines. Plateaux at 1 km (Western Anatolia 1), 2 km (Eastern Anatolia 2), 3 km (Tien Shan 3) and 5 km (Tibet 5). Box in Eastern Turkey shows the area of Figs 8 and 9. Inset illustrates the fundamental structural problem of wide convergent plate boundary zones that, although the displacement (D) and displacement rate ($\dot{D}$) between opposing forelands may be known, the way in which these are converted into convergent strain (ϵ) and strain rate ($\dot{\epsilon}$) may be very complicated. A and B are lines of schematic section shown in Fig. 2. A, Aegean; HP, Hungarian Plain; T, Tyrrhenian.

complex and variable strains and smaller block-bounding displacements. This contrasts with oceanic plate boundaries, which are generally narrow, relatively simple zones in which only a small portion of relative plate motion is converted into strain and smaller displacements (McKenzie 1972). This contrast is probably due to the relative weakness and buoyancy of quartz and the relative strength and negative buoyancy of olivine as the principal mineral phases in the continents and oceans respectively. Also, the great inhomogeneity and anisotropy of the continental crust, riddled with zones of low strength, generated and modified by many varied mechanisms, contrasts with the relative homogeneity of the oceanic lithosphere generated by plate accretion with fracture zone modifications (Dewey 1982).

A basic problem of collisional tectonics is how relative plate displacement directions and rates are converted in strains and strain rates within the convergent plate boundary zone (Fig. 1). Our understanding of this problem, although incomplete, has progressed greatly since Argand (1924) first explained the Himalayan Orogen as a result of simple underthrusting of India beneath Asia, a mechanism advanced today by Powell & Conaghan (1973) Barazangi & Ni (1982), Ni & York (1978) and Ni & Barazangi (1984), among others, to explain the thick Tibetan crust (Chen & Molnar 1981; Molnar & Chen 1983). Two further competing models have been suggested to explain the Tibetan Plateau (Fig. 1). Molnar & Tapponnier (1975, 1977a,b, 1978, 1979, 1981), Tapponnier & Molnar (1976, 1977) and Tapponnier *et al* (1981, 1982) have advanced a horizontal plane strain slip-line solution to explain the pattern of strike-slip wedging and E–W extension in Tibet generated by peninsular India behaving as a rigid indenter. Horizontal plane strain alone, however, cannot explain the thickened Tibetan crust (> 80 km). An alternative view is that the Tibetan lithosphere is shortened and thickened by vertical stretching (Dewey & Burke 1973). We do not imply a particular mechanism for vertical stretching, only that the crust is thickened by mechanisms, perhaps subhorizontal shearing and thrusting, operating on a smaller than crustal scale. England & McKenzie (1982) have argued for a viscous continuum model whereby the progressive impingement of the rigid Indian lithosphere has caused vertical stretching over a progressively increasing area of Asia. In their model, vertical stretching is buffered at about 80 km by lateral spreading of the thickened crust at an Argand Number (ratio of stress caused by crustal thickness difference and stress needed to continue convergence, England & McKenzie 1982) of 3. This model has the particular merit of explaining E–W lateral wedging and extension as a late stage consequence of crustal thickening.

The Tibetan Plateau is the higher and larger of the two major plateaux in the Alpine/Himalayan system (Fig. 1), the other being the Turkish/Iranian Plateau, a zone of lithospheric horizontal shortening about 2 km above sea level (Şengör & Kidd 1979). Such plateaux, with roughly constant mean elevation, are one of five tectonic components in collisional systems (Figs 1 and 2), namely plateaux, thrust belts, foreland lithospheric flexures, widespread foreland/hinterland deformation zones and orogenic collapse/distension zones. We here define foreland and hinterland to mean those regions exterior to the outermost major overthrust belts in the direction and away from the direction, respectively, of principal orogenic vergence. Thrust belts and foreland flexures are common to all collisional systems, whereas plateaux, widespread foreland/hinterland deformation and collapse zones may or may not be present in a particular portion of the orogen.

Thrust belts develop principally where the thinned continental crust of a rifted margin is progressively restacked and thickened toward the foreland. This commonly involves thrust rejuvenation of old listric normal faults (Jackson 1980) and thrust shortening is usually initially below sea level before the crust is restacked to 30 km. The oldest, highest, internal, basement-cored nappes are generally discontinuous along orogenic strike, whereas younger, exterior foreland thinner-skinned fold–thrust belts are continuous and highly cylindroidal (Fig. 3). Where detachment occurs along a weak horizon within a foreland sequence, rocks above the detachment can shorten significantly independently of the basement for foreland distances of 400 km (Geiser & Engelder 1983). The higher internal nappes commonly carry sub-continental mantle and complete, but thin, crustal sections (Fig. 4), crustal thinning dating from the time of crustal extension and separation. Tectonic shaving thins the highest nappes and the resulting slices (e.g. the Sesia Zone in the Alps) may be subducted to the blueschist facies (Fig. 4). Metamorphic patterns in thrust belts generally involve a localized blueschist overprint of older crustal patterns overprinted in turn by a regional amphibolite/greenschist pattern (Fig.

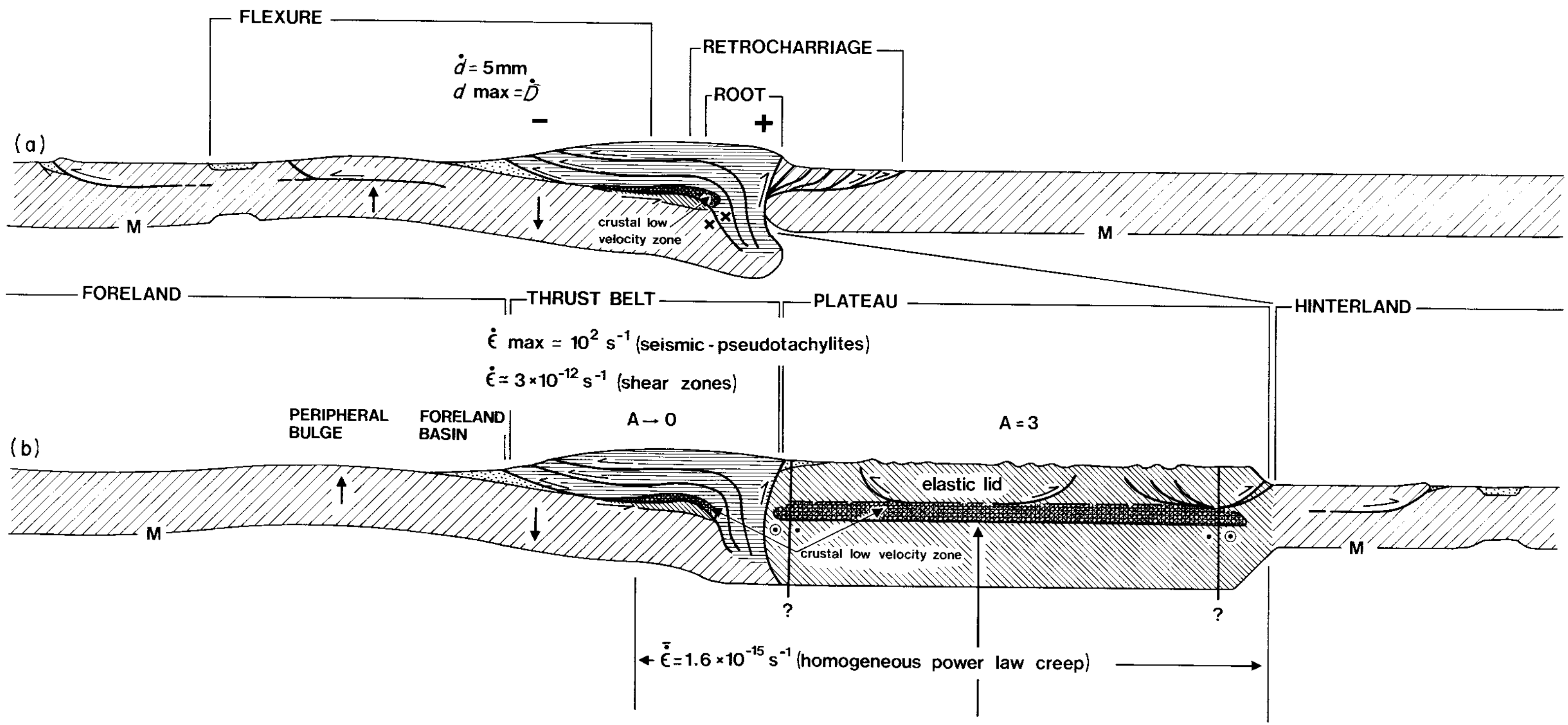

FIG. 2. Schematic orogenic sections showing the elements of collisional orogens (a, Alpine type; b, Himalayan/Tibetan type). Minus and plus symbols refer to isostatic gravity anomaly pairs. Foreland/hinterland crust: oblique lines; thickened crust of plateau: fine oblique lines; thrust sheets: horizontal lines. Symbols as in Fig. 1, A represents Argand Number (England & McKenzie 1982).

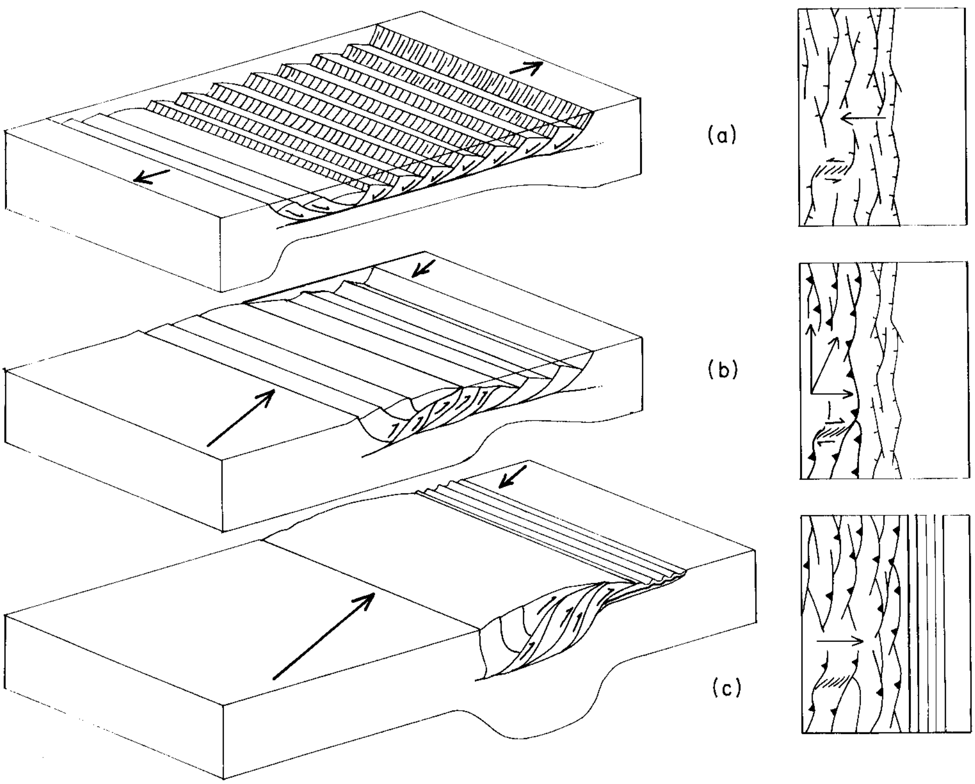

FIG. 3. Block diagram and plan views of the extension of the upper continental crust by listric normal faulting (a) followed by the progressive restacking of the crust (b,c) by thrust faults nucleated on the earlier extensional faults. Arrows indicate extension (a) and convergence (b,c) direction of foreland and hinterland.

4). The innermost highest nappes and adjacent ophiolitic or cryptic suture zones are usually steepened to overturned in late-stage crustal scale rotation or *rétrocharriage* zones (Roeder 1979) that may involve extensive backthrusting over adjacent plateaux or hinterlands (Figs 2 and 4). Crustal low-velocity zones occur in thrust belts (Alps: Rybach *et al.* 1980) and plateaux (Tibet: Chen & Molnar 1981) (Figs 2 and 4) and are discussed in a later section.

Foreland flexure involves the springboard-like downbending of the lithosphere by the vertical load of the advancing thrust sheets, to form a foreland basin, with a corresponding outer arch or peripheral bulge, the wavelength and amplitude of which depends on the flexural rigidity and, in turn, thermal age of the lithosphere (Karner & Watts 1983) (Figs 2 and 4). The Indo-Gangetic Foredeep of the Himalayas and the associated peripheral bulge are long wavelength flexures superposed on Archaean lithosphere modified, in the Himalayan Thrust Belt, by Triassic rifting. The Swiss Plain Foredeep and associated peripheral bulge of the Massif Central/Vosges/Black Forest/Bohemian Massif are of shorter wavelength superposed on a Hercynian lithosphere modified by Jurassic extension and Eocene rifting.

The widespread foreland deformation of NW Europe (Dewey 1982) and hinterland deformation of Asia (Molnar & Tapponnier 1975), in response to Alpine and Himalayan collisions respectively (Fig. 1), show that the stresses generated by continental convergence can affect continental portions of plates hundreds, even thousands, of km from the thrust belt; these stresses may have been enhanced by ridge push from the Mid-Atlantic Ridge and from the Indian Ocean Ridge. The degree and extent to which forelands deform, or whether the hinterland or foreland takes up part of the

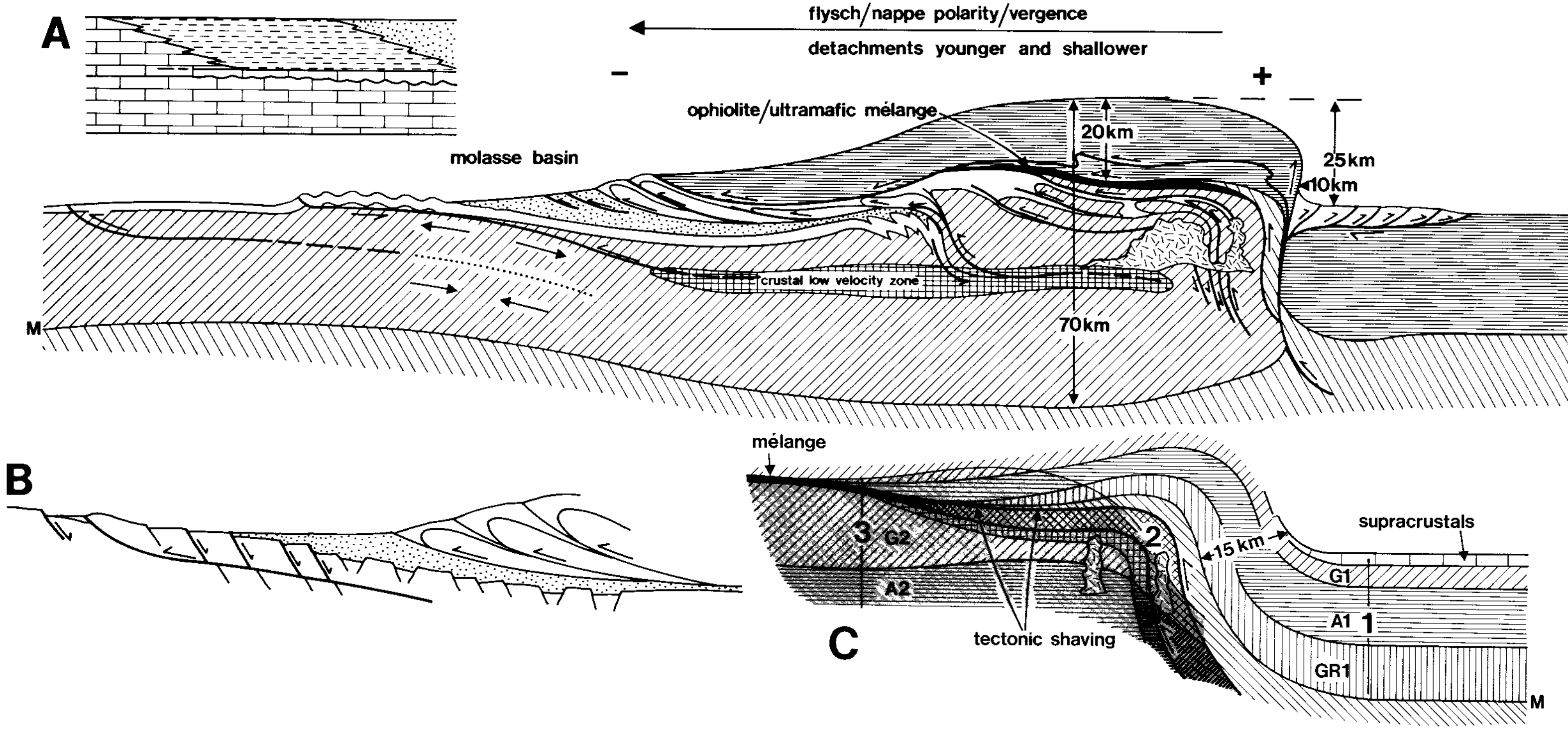

FIG. 4. Schematic but true-scale section through a thrust orogen based specifically and in detail upon the Swiss/Italian Alps (Rybach *et al.* 1980). (a) Schematic stratigraphy of the shelf and foreland basin of a thrust orogen showing disconformity resulting from the early outward migration of the peripheral bulge. (b) Extensional structures beneath the foreland basin resulting from flexural extension cut by a thrust detachment. (c) Metamorphic overprints; 1: original metamorphic sequence of pre-orogenic crust (GR, granulite; A, amphibolite; G, greenschist); 2: blueschist overprint associated with shaved tectonic slices formed during the early phases of restacking; and 3: thermal overprint.

convergence, appears to depend upon the thermal age and anisotropy of the lithosphere. The preferential hinterland deformation of Asia, rather than the Indian Foreland, is probably because the Tibetan lithosphere was warmed and thinned by pre-collisional Mesozoic/Early Tertiary subduction and because the Asian lithosphere is a complex inhomogeneous assemblage of Hercynian blocks, arcs and accretionary wedges whereas the Indian lithosphere has mainly an Archaean basement age.

Extensional collapse zones occur principally in the Alpine/Mediterranean region (Aegean, Tyrrhenian and Pannonian Basins, Fig. 1). These depressions may have a similar origin to each other. Royden *et al.* (1983) have invoked subducting slab rollback (Dewey 1980) of the European Foreland for the extension of the Pannonian Basin, a back-arc mechanism that could also explain the Tyrrhenian and Aegean Basins.

A notable feature of the Alpine/Himalayan convergent zone is that, although the convergence rate varies from 10 to 50 mm yr^{-1}, and the width of the deforming zone, as defined by earthquake distribution, ranges from a few hundred to several thousand km, the spatial average convergent strain rate is roughly constant along the belt at about 1.5×10^{-15} s^{-1}. Ben-Avraham & Nur (1976) have suggested that the width of the zone is proportional to the convergent displacement rate, that is the rate at which material is fed into the convergent zone. If the same cross-sectional area of material was involved in the zone of shortening, with time the strain rate would rise exponentially. A constant width-shortening zone maintains a constant strain rate. The geological evidence from many orogens indicates that material enters convergent strain zones in the shortening direction with time because thrusts prograded into hitherto undeformed crust.

Crustal rheology and detachment

Many lines of evidence are gathering, that in convergent zones, the upper crust forms a high-strength layer from 5 to 15 km thick, that may be thrust for hundreds of km as a thin plate or a series of stacked flakes. In the Southern Appalachians, a thin sheet involving the Blue Ridge and Inner Piedmont has moved westwards over the foreland for at least 300 km (Cook *et al.* 1979). Similar detachments are deduced in Pakistan from earthquake hypocentres (Armbruster *et al.* 1978). In California, in the region between Bakersfield and Riverside, where the San Andreas Fault is in a transpressional locking orientation, upper-crustal flakes up to 15 km thick (hypocentres shallower than 15 km) have detached from the lower crust to offset the San Andreas Fault in cross-section and to cause southwestward over-thrusting of the San Gabriel Mountains and Transverse Range. Also, a Mohave 'wedge' is moving eastwards from the San Andreas/Garlock convergence. Rotation of crustal flakes up to 90° (Luyendyk *et al.* 1980) has occurred at the edges of which upper-crustal basins, such as the Ridge Basin, have opened. The sense of rotation along the Cordilleran margin of North America is clockwise (Beck 1976), consistent with dextral motion along the margin between Pacific and North American Plates. The structural and palaeomagnetic evidence appears to suggest that most, if not all, of these flakes have undergone rigid body rotation, i.e. external rotation rather than internal viscous rotations. However, a critical question, which we address for Eastern Anatolia in a later section, is to what extent is strain, at various structural levels in the crust, continuous or discontinuous in space and time in continental convergence zones and, where fault-bounded blocks or flakes can be observed, to what extent are they internally rigid with strain confined to narrow slip zones at their boundaries.

It is likely that such flakes are the surface expression of thin upper-crustal sheets above intracrustal *décollements* rather than small 'platelets' because the latter would be mechanically difficult and unlikely narrow lithospheric 'spindles'. The kinematic theory of strains, rotations and displacements in complex continental convergent plate boundary zones has been addressed by McKenzie & Jackson (1983) and will not be considered here.

The depth frequency of hypocentres (Meissner & Strehlau 1982) is a guide to the thickness of an upper brittle or elastic layer in which stress accumulation and release by faulting and jointing occurs. Hypocentral frequency, magnitude and highest stress drop reach maxima (Das & Scholz 1983) at depths from as little as 5 km in extensional areas of high heat flow to as much as 20 km in convergent areas of low heat flow (Fig. 5). This indicates an inverse relationship between heat flow and hypocentral depth maxima which, in shield areas, is related to crustal stabilization or lithospheric thermal age (Chen & Molnar 1983). In some regions (Chen & Molnar 1983), a seismic gap exists in the lower crust between upper- and middle- crustal hypocentres and

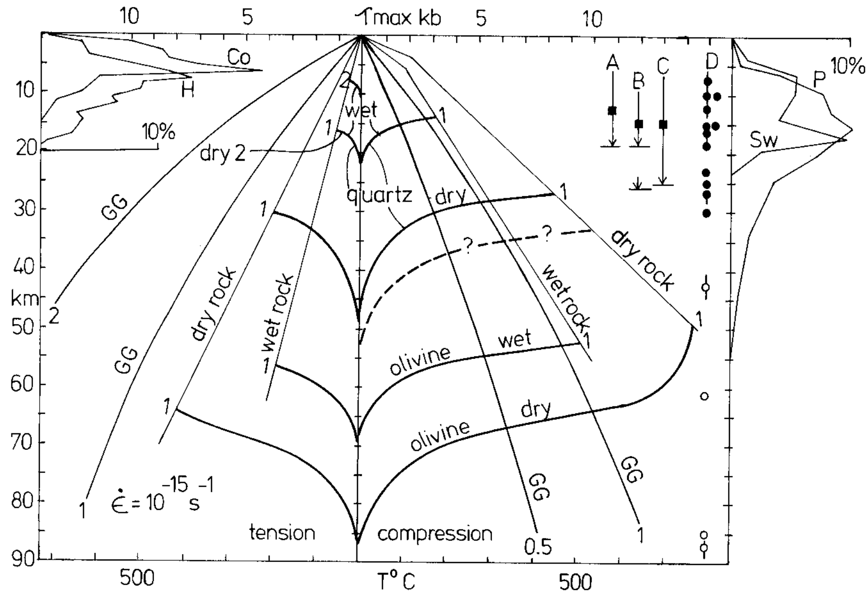

FIG. 5. Shear strength of wet and dry quartz and olivine in extension and compression at a strain rate of 10^{-15} s^{-1}, at heat flows for geothermal gradients corresponding to 1 and 2 HFU, modified and extrapolated from Meissner & Strehlau (1982) and Kirby (1980). Dry rock and wet rock curves refer to the brittle shear strengths (Byerlee 1968). Depth frequency distribution of hypocentres; SW, Schwarzwald; Co, Coso; H, Haicheng (Meissner & Strehlau 1982); P, Pakistan Himalayas (Armbruster *et al.* 1978); D, continental convergence zones (open circles, mantle hypocentres); A–C, continental interiors (square gives mean, line gives range) with basement ages of 250–800 Ma, 800–1700 Ma and greater than 1700 Ma, respectively (Chen & Molnar 1983). Temperature scale refers to geothermal gradients (GG) with surface heat flows 1 and 2 in HFU. Typical stress-drops of only a few hundred bars indicate that these theoretical strength profiles must be regarded only as maxima, for flawless materials.

upper-mantle hypocentres. The maxima correlate well (Fig. 5) with strength predictions from extrapolated experimental data. Byerlee (1968) showed that, at low temperatures, the coefficient of friction and hence fracture and sliding strength of most materials is proportional to confining pressure and therefore to depth. Shearing strength for dry and wet rocks in compression and extension are plotted as a function of depth in Fig. 5. However, the shear strengths of rocks and minerals at higher temperatures are extremely temperature-, rather than pressure-, dependent. At any given temperature, the creep strength of quartz, the principal crustal phase, is very much less than that of olivine, the principal mantle phase (Fig. 5). Also, hydrous mineral assemblages are weaker than anhydrous. For dry or wet, quartz- or olivine-dominated mineral assemblages, strength maxima exist at the fracture/creep envelope intersection (Fig. 5). The role of feldspar, a possible stress-bearing phase in some lower crusts, is uncertain, except that petrographic textural evidence indicates that it is stronger than quartz in the upper greenschist, amphibolite and granulite facies. A great range of petrological crustal profiles exist (Dewey & Windley 1981) involving various combinations of hydrous and anhydrous quartz and feldspar dominated assemblages in a wide range of metamorphic grades. In Fig. 6, a wet quartz/dry quartz/dry olivine profile, for a heat flow of 0.75 HFU and a strain rate of 10^{-15} s^{-1}, has been chosen to roughly match the depth frequency for earthquake hypocentres (Jackson & McKenzie 1984) in the Turkish/Iranian Plateau. This gives three strength maxima and minima corresponding to wet and dry quartz as upper and lower layers in a 50 km crust and dry olivine in the upper mantle. The segmentation of the upper high-strength layer or elastic lid (Dewey 1982) is the likely origin of upper-crustal flakes within which a wide variety of detachment surfaces are possible (Fig. 6). The strength minima are probably zones of ductile strain in which constructive metamorphic fabrics are generated in rather high-pressure/low-temperature metamorphic facies with no

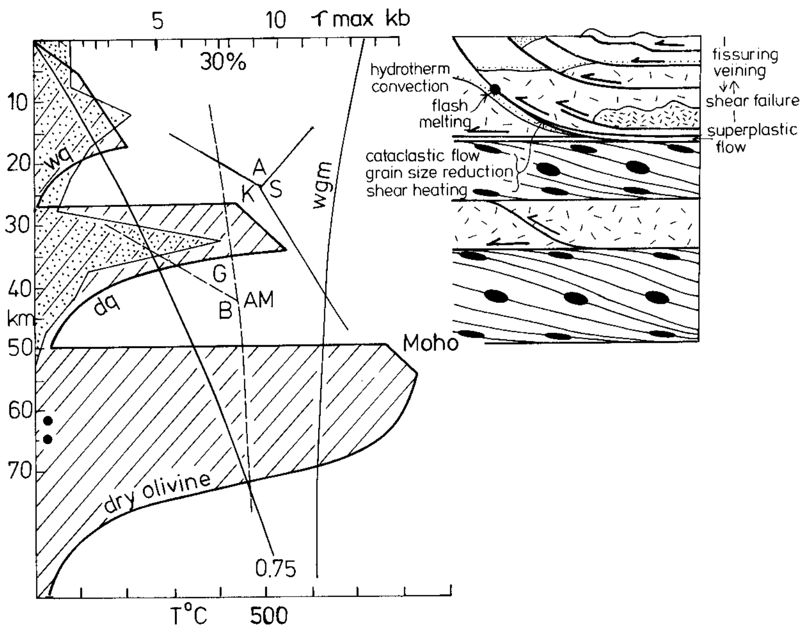

FIG. 6. Strength profile (enveloping obliquely striped area) for a 50 km continental crust in compression comprising a 27 km thick upper hydrous crust (wq, wet quartz), a lower anhydrous crust (dq, dry quartz), and a dry upper mantle at a strain rate of 10^{-15} s^{-1} and for a geothermal gradient corresponding to a surface heat flow of 0.75 HFU. Stippled area: depth/frequency distribution of hypocentres from Jackson & McKenzie (1984). A, andalusite; AM, amphibolite; B, blueschist; G, greenschist; K, kyanite; S, sillimanite; wgm, wet granite melting.

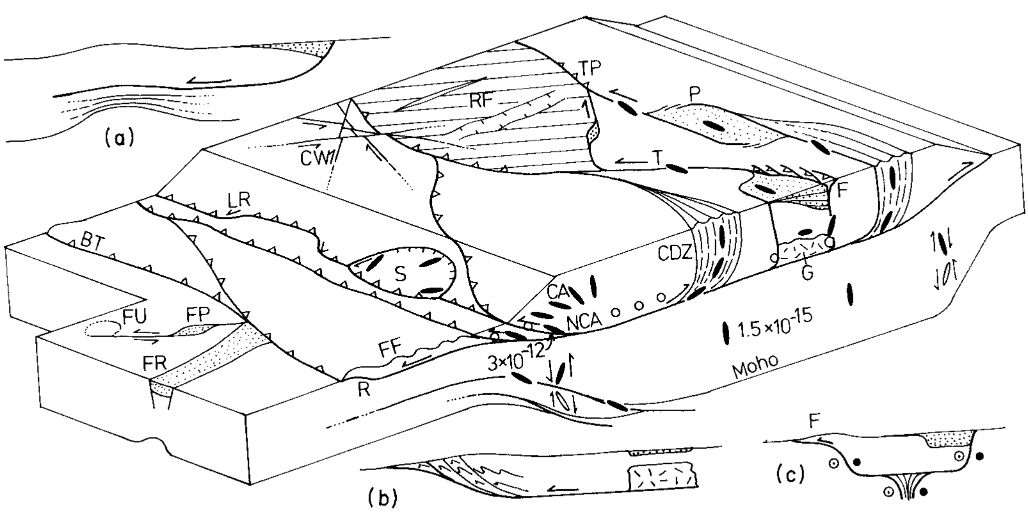

FIG. 7. Schematic illustrations of the strains and displacements in a collisional zone. (a-c) Modes of detachment termination referred to in text. BT, basement thrust; CA, coaxial strain; CDZ, convergent deformation zone; CW, conjugate wrenching; F, flower structure; FF, foreland folding; FP, foreland pull-apart; FR, foreland rift; FU, foreland uplift; G, granite; LR, lateral ramp; NCA, non-coaxial strain; P, pull-apart; R, ramp; RF, rigid flake; S, surge zone; T, transform; TP, transpression; small circles: hypocentre of large earthquakes. Ellipses indicate finite elongation/ shortening directions. In (c) open and filled circles indicate respectively motion away from and towards the observer.

crustal partial melting (Fig. 6). This is consistent with field structural evidence that, with increasing metamorphic grade (depth), deformation becomes more homogeneous on a smaller scale. At high structural levels, strain is partitioned and concentrated on narrow high strain rate (10^{-12} s^{-1}, Barton & England 1979) slip zones while, at deeper levels, strain is more penetrative. In later sections, we take the profile of Fig. 6 as the basic model for the East Anatolian Convergent Zone.

Elastic lid or flake detachment, especially where rotations about vertical axes occur, leads to complicated compatibility problems at flake margins. This is well seen in Anatolia as shown below and is particularly evident in the Transverse Ranges of California where substantial localized pull-apart basins and thrust zones occur on a restricted geographic scale at flake boundaries and triple junctions.

Local termination of basal flake detachments offers a possible explanation for a wide variety of localized crustal structures, which may be arranged in various of geometrical combinations. These may comprise listric extensional detachments passing laterally into zones of lower-crustal stretching with resulting pop-ups (Fig. 7a), batholiths with mid-crustal flat bases (Lynn *et al.* 1981) passing laterally into thrust zones (Fig. 7b), and rotated flakes with marginal flower structures above detachments that relay transform motion laterally into wide lower-crustal and mantle shear zones. Figure 7 summarizes schematically the range of crustal structures characterizing collisional orogens and their forelands, most of which occur in Eastern Anatolia and are described in a later section.

Eastern Anatolia is a well-exposed and accessible present-day collisional convergent zone (Fig. 8) forming a plateau averaging some 2 km above sea level. It may be one of the best areas in the world to study the geometry and kinematics of continental convergence. The E Anatolian Convergent Zone (EACZ) is a region of frequent and widespread earthquakes (Fig. 9) ranging up to $M = 8$ (Ergin *et al.* 1967; Canitez & Ucer 1967b; Dewey 1976; Buyukasicoglu 1979; Jackson & McKenzie 1984) and measurable deformations and displacements are visibly occurring throughout the region. The region is an aggregate of arcs, blocks and accretionary prisms and is characterized by great structural complexity. The present (neotectonic) phase of collisional convergence began about 12 Ma ago in which the northwards convergence of Arabia with Eurasia produced shortening and thickening of the crust and caused a wedge-shaped Anatolian 'block' to migrate westwards over the subducting oceanic lithosphere of the Eastern Mediterranean. We have been studying Anatolian neotectonics for the past 10 years and a preliminary outline of our conclusions is presented below.

Collisional assembly of Anatolia

Four major tectonic subdivisions of Turkey were defined by Ketin (1966a). The 'Central Anatolian Massifs' (Menderes Massif, Kirşehir Massif) of Central and Western Turkey and the 'Anatolides' are now regarded as Alpine structures (Ketin 1966a; Durr *et al.* 1978) and not Hercynian or older *Zwischengebirge* (Brinkmann 1976) within the Anatolian Orogen. Several workers have argued that the Central Turkish Anatolides and the Southern Turkish Taurides formed a single palaeogeographic realm during the entire Mesozoic and Tertiary, characterized mainly by Triassic–Neogene shelf carbonates although, in the internal parts (Anatolides), sedimentation ended earlier (Ricou *et al.* 1975; Ozgul 1976; Durr *et al.* 1978). The non-metamorphic, mildly deformed part of this carbonate platform is exposed beneath large composite nappes especially in the Western Taurus (Brunn *et al.* 1971; Bernoulli *et al.* 1974; Delaune-Mayere *et al.* 1977). It has a great along-strike continuity westwards into the external units of the Hellenides and eastwards into Iran (Ricou *et al.* 1975).

During the Late Cretaceous, part of the ocean floor separating the Anatolide/Tauride Platform from the Northern Turkish Pontides was obducted onto the former (Ricou *et al.* 1975). The Pontides, connecting the Rhodopian Massif and the Srednogorie province of the Balkan Ranges (Hsü *et al.* 1977) with the Lesser Caucasus (Adamia *et al.* 1977) formed, at this time, a S-facing island arc S of an opening Black Sea marginal basin. The Pontides have Late Cretaceous–Palaeogene

FIG. 8. (*Opposite*). Neotectonic map of the E Anatolia Convergent Zone (EACZ) and its Arabian Foreland showing fractures (fine lines), mapped faults (thick lines), young basins (dotted), volcanoes and volcanic fields (areas limited by thick dotted lines, thrusts and folds that have been active during the past 12 Ma). Encircled dots and small black circles are the epicentres of very large (M>7) and large (M>6) earthquakes, respectively.

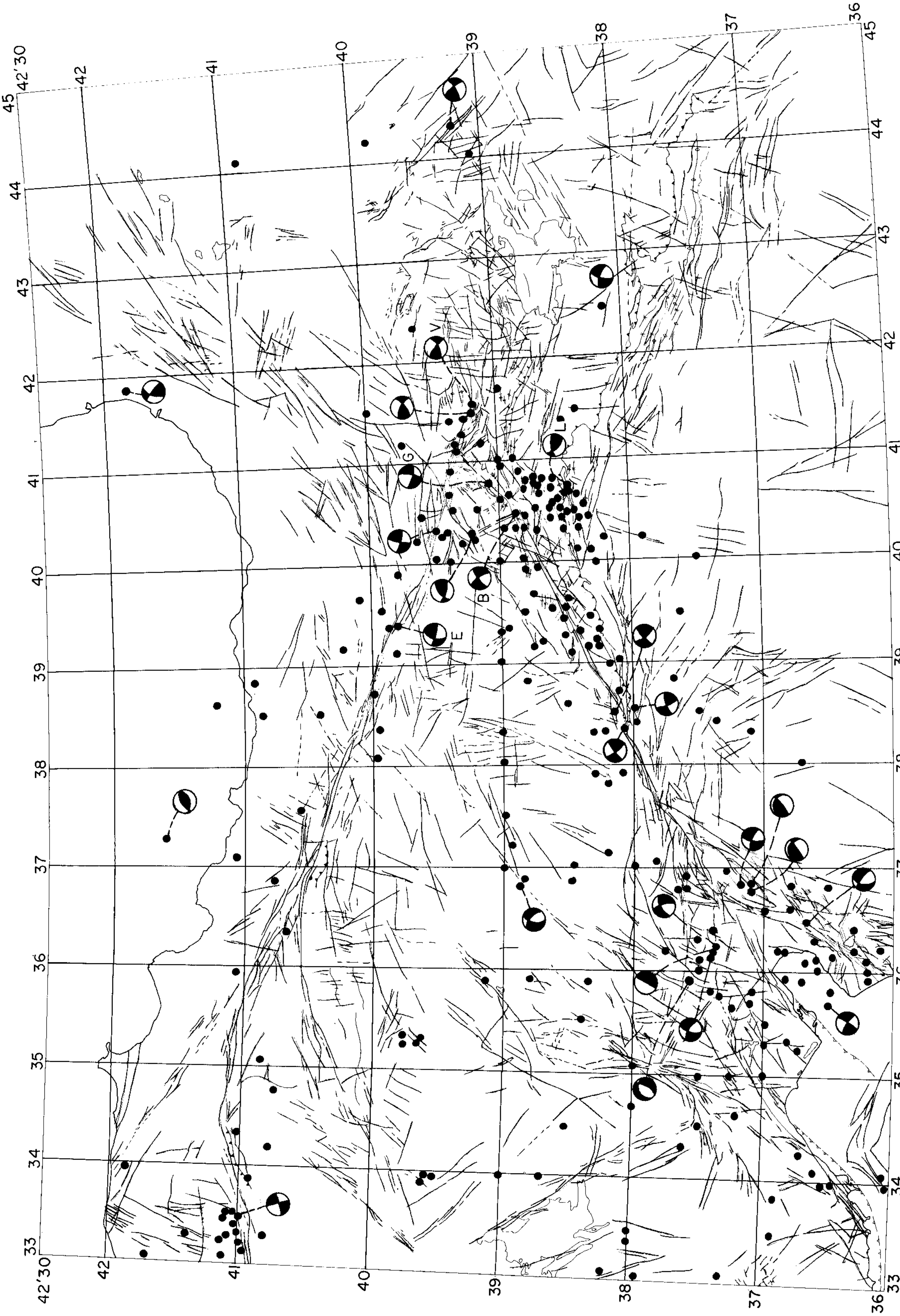

FIG. 9. Epicentres of E Anatolian earthquakes of $M>5$ and selected nodal plane solutions from Buyukasicoglu (1979). B, Bingol; E, Erzincan; G, Goynuk; L, Lice; V, Varto.

calc-alkaline magmatism (MTA 1962; Tokay 1973; Seymen 1975) and widespread Late Cretaceous–Palaeocene ophiolitic mélange accumulation (Tokay 1973; Gansser 1974; Seymen 1975; Bergougnan 1976). That both calc-alkaline magmatism and mélange accumulation in the Pontides continued long after the Cretaceous obduction of the ophiolites onto the Anatolide–Tauride Platform, rules out a Late Cretaceous Pontide–Anatolide collision proposed by Ricou *et al.* (1975). The uplift of the Pontide–Anatolide Suture (Lutetian plant fossils NE of Ankara; Tokay 1973) and the initiation of major imbrication and S-vergent thrusting accompanied by the rapid formation and southerly migration of flysch-molasse troughs in the Anatolide–Tauride region during the Early Eocene (Delaune-Mayere *et al.* 1977), are evidence for Eocene Pontide–Anatolide collision at least in the western section of Anatolia. In the E, the collision may not have occurred until the Burdigalian (Seymen 1975). After the collision, the Anatolide–Tauride realm was further imbricated and stacked and high *T/P* metamorphism and anatexic granite plutonism affected the internal Anatolides (Durr *et al.* 1978).

In SE Anatolia, the Bitlis Ocean had been in existence since the Late Triassic (Dewey *et al.* 1973; Bein & Gvirtzman 1977). From Early Cretaceous to the Middle Miocene, it was also consumed along a N-dipping subduction zone (Dewey *et al.* 1973; Hall 1976; Dewey & Şengör 1979) and was completely obliterated by a Late Miocene collision along the Bitlis Suture.

In latest Serravallian, earliest Tortonian time, about 11.8 Ma ago, a fundamental palaeogeographic, sedimentological and tectonic change occurred throughout Eastern Anatolia (Fig. 10) that, we believe, resulted from the final collisional closure of the Bitlis oceanic tract and accompanied the beginning of widespread crustal shortening and the beginning of uplift across Eastern Anatolia. Throughout the region, Serravallian shallow marine sediments give way to terrestrial sediments intermittently and patchily deposited in a wooded seasonal savanna environment. In the southern border thrust zone, the Tortonian Lice Flysch signified the beginning of thrust loading. Tortonian Kythrean Flysch follows the Serravallian deposition of *Globerigina* marls in the Eastern Mediterranean, witnessing the emergence of a nearby source area. The Central Anatolian ova regime, characterized by large, rather equant, fault-bounded depressions (ovas) with Neogene

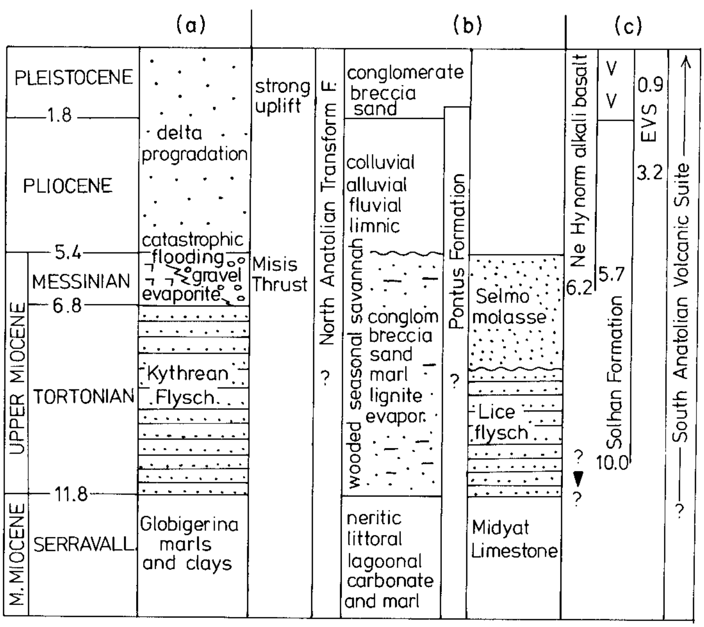

FIG. 10. Summary of the medial Miocene to present-day events in the Eastern Mediterranean region. (a) Eastern Mediterranean; (b) Eastern Anatolia (sediments and tectonics); and (c) Eastern Anatolia (volcanism). Stratigraphic divisions and ages from Rogl & Steininger (1983). Volcanic data mainly from Innocenti *et al.* (1976).

terrestrial sediments and, locally, young basaltic volcanics began during the Late Miocene. Thus, by Late Miocene times, the composite Anatolian Orogen had already been assembled more or less in its present configuration. Since Late Miocene, there has been continuous continental lithosphere between the converging Arabian and Eurasian Cratons in Eastern Anatolia, whereas, in Western and Central Anatolia, the Anatolian Wedge has been facing the underthrusting oceanic lithosphere of the African Plate.

Displacement and strain in Eastern Anatolia

In a detailed study of earthquake epicentres and focal mechanism solutions, McKenzie (1972a,b) postulated that the convergence of Arabia northward into Eurasia is forcing the wedge-shaped Anatolian Block westward. This movement is accommodated along the right-lateral N Anatolian Transform Fault (NATF) and its complement, the left lateral E Anatolian Transform Fault (EATF). To the E, lies the E Anatolian Convergent Zone (EACZ). To avoid excessive thickening by shortening, the EACZ 'wedged-out' a considerable piece of the Anatolian Orogen along two new boundaries, the N and E Anatolian Transform Faults, towards the more readily subductable oceanic region of the Eastern Mediterranean (McKenzie 1972a,b; Dewey & Şengör 1979), thereby giving birth to the Anatolian 'Block' or 'Wedge'.

Epicentre maps by Ergin *et al.* (1967) and Buyukasikoglu (1979), studies of foreshock–mainshock–aftershock sequences of large earthquakes (Dewey 1976), airphoto and Landsat interpretation (Allen 1969, 1975; McKenzie 1976), field studies (Wallace 1968; Arpat & Saroglu 1972) and regional geologic synthesis (Dewey & Şengör 1979) support this interpretation. Regional geology suggests that suturing between the Arabian Platform and the Anatolide/Tauride Platform within the Bitlis Suture Zone was completed in the Late Miocene (Dewey & Şengör 1979).

The style and geometry of strain and displacement in the EACZ is summarized in Figs 8 and 9. Figure 8 shows the distribution of neotectonic faults and folds within the EACZ compiled mostly from field studies, interpretation of Landsat images and airphotos and from published maps. Figure 9 is a compilation and replotting of earthquake epicentres and focal mechanism solutions. In this section, we describe the structure and history of the NATF, EATF and EACZ and reference should be made throughout to Figs 8 and 9. We have much more data for the NATF than for the EATF, reflected in the much longer ensuing section on the former.

North Anatolian Transform Fault (NATF)

The NATF is one of many large strike-slip faults, striking at low angles to the general trend of the Alpine–Himalayan system of Eurasia and forming late in the orogenic history of the segments they cut (e.g. Insubric Line of the Western Alps (Gansser 1968; Trumpy 1973; Laubscher 1971); Pustertal Line of the Eastern Alps; Kraistide–Vardar Lineament of the Balkan–Hellenide Chain (Laubscher 1971; Boncev 1974); Zagros Fault of SE Iran (Berberian 1976); Karakorum Fault of the W Himalaya–Karakorum (Molnar & Tapponnier 1975)). These faults appear to be closely related to the disintegration of colliding promontories and change in direction of relative motion along the suture after collision.

The seismically active NATF is a right-lateral fault zone taking up the relative motion between the Black Sea and the Anatolian 'Block' and is sub-parallel to the Black Sea coast of Anatolia running some 1200 km from Karliova in the E to the Gulf of Saros in the W, thereby connecting the EACZ (McKenzie 1972a,b; Şengör 1977; Şengör & Kidd 1979) with the western end of the Hellenic Trench through the complex plate boundary zone of the Aegean (Dewey & Şengör 1979). This definition is that of Allen (1969) and McKenzie (1972a,b) and is not equivalent to the N Anatolian earthquake fault (Kuzey Anadolu Deprem Fayi) of Ketin (1957) and the N Anatolian strike-slip fault (Nordanatolische Horizontalverschiebung) of Pavoni (1961a) and Ketin (1969, 1976), who believed it to continue into Iran.

The NATF, Nowack's (1928) Paphlagonische Narbe, Salomon-Calvi's (1936a, 1940) Fortsetzung der Tonale-Linie and Pamir's (1950) Cicatrice Nord-Anatolienne, was believed to be the vertex of the Alpine Orogen in Anatolia. Salomon-Calvi (1936a, 1940) viewed it in the context of Wegener's theory of continental drift and, following Argand (1924), regarded it as the suture between collided Gondwanan and Eurasian elements. A series of disastrous earthquakes along the NATF, beginning with the Tercan earthquake on 21 November 1939 and the Erzincan catastrophe on 28 December 1939, began a phase of detailed observations (eg. Pamir & Ketin 1940, 1941; Parejas *et al.* 1942; Pamir & Akyol 1943;

Blumenthal 1945a,b). Ketin (1948) concluded that the earthquakes occurred on an active right-lateral, strike-slip fault zone that extended along the entire length of the Black Sea mountains of N Turkey and showed that this structure post-dated the main orogenic structure of Turkey. Ketin (1948) interpreted it as a young feature along which an Anatolian Block, S of the fault, is moving westwards with respect to the Black Sea and argued that a complementary left-lateral, strike-slip fault must bound the Anatolian Block to the S, citing the Kozan earthquake in SE Turkey as supporting evidence. Ketin & Roesli (1953) compared the NATF with the San Andreas Fault of California.

In several recent plate tectonic interpretations of the Eastern Mediterranean, the NATF plays an important role (McKenzie 1972a,b; Tapponnier 1977; Dewey & Şengör 1979). The NATF and analogous strike-slip faults in collision environments are key elements of recent models of continental collision processes (Molnar & Tapponnier 1975; Şengör 1976; Dewey 1977). Thus, the detailed tectonic evolution of the N Anatolian Transform is of great importance, especially its age, slip rate and cumulative offset, to be able to test and improve such models.

Like most of the large, active, strike-slip faults of the circum-Pacific region (Allen 1965) or Central Asia (Molnar & Tapponnier 1975), the NATF has an extremely well-developed surface expression for most of its length. It is defined by a sharp 'rift morphology' delineating a broad fault zone up to 1 km wide composed of numerous sub-parallel and anastomosing faults, offset, captured and dammed streams, sag ponds and elongate island-like hills within major valleys following the course of the fault zone. Earthquakes have caused sizable landslides; lakes formed by landslide damming, are common along the course of the fault (Pamir & Ketin 1941).

Morphologically, the NATF can be followed as a fairly continuous, strike-slip fault zone from Karliova to about Mudurnu. East of the point where it joins the EATF, about 10 km E of Karliova, it is lost in the block fault and thrust terrane of the EACZ. Although several earthquakes E of Karliova (e.g. at Varto: Ambraseys & Zatopek (1968), and Caldiran: Arpat & Iz (1977); Toksoz *et al.* (1977)) produced right-lateral, surface breaks, they lack the continuity and uniformity of the NATF breaks and resemble the irregular and discontinuous strike-slip faults of NW Iran (Berberian 1976). Also, many of the earthquakes E of Karliova have thrust components in contrast to the pure strike-slip earthquakes along the NATF (McKenzie 1972a,b). From Karliova, the NATF is continuous to Erzincan, where it jumps for about 10 km to the N across the extensional Erzincan Plain, a typical pull-apart basin (Crowell 1974), characterized by young sediments and small basaltic volcanoes (Ketin 1976). From Erzincan to Resadiye, the trace of the fault zone is again continuous; the characteristic morphological features of this segment are elongate sag ponds, springs sometimes associated with travertines, fault scarps cutting the alluvium in the valley floor (related to the 1939 Erzincan earthquake) and deformed stream valleys (Seymen 1975). To the W of Erzincan, recent anticlines within Pliocene sediments have strong morphological expression (Tatar 1975). Between Resadiye and Erbaa, the continuity of the fault is again lost and, whereas the trace coming from Erzincan turns into an E–W orientation S of Amasya, a new trace begins to the N of Resadiye. Between the southern and northern branches, a third branch appears to be a secondary extensional feature within a broad pull-apart basin similar to the Erzincan Plain. Seymen (1975) has mapped this region in detail and shown that this extensional feature is also the locus of Recent basaltic volcanism. He showed that, on both sides of the Kelkit Valley, which here follows the main southern branch of the N Anatolian Transform Fault, the ridges bounding the auxiliary stream valleys are bent in a clockwise (dextral) sense.

The Niksar Basin is a Pliocene–Quaternary sedimentary basin located along the NATF NE of Ankara. The main trace of the NATF is offset approximately 10 km across this pull-apart basin. East of the basin, the fault occurs as a single, well-defined trace. This breaks into a complicated series of poorly defined faults in the vicinity of the Niksar and adjacent Erbaa Basins. Both the NE and SW walls of the Niksar Basin are characterized by a series of broad terraces which are fairly continuous laterally and which generally dip gently (up to 20°) on the SW wall towards the interior of the basin. The NW margin of the basin has an *en échelon* set of E–W steeply dipping to vertical faults approximately parallel with the main fault trace to the E. Motion on these faults appears to have had both normal (S side down as evidenced by the offset of an erosion surface between Early and Late Cretaceous carbonates) and right-lateral, strike-slip components. Structures along the SW margin of the basin are similar, except that the sense of vertical offset on faults is N side down.

Generally, the NATF forms a wide belt of numerous, sometimes parallel, sometimes anastomosing, strike-slip faults. Canitez (1962) has shown, on the basis of seismic and gravity observations, that the crust beneath the fault zone is thinner than normal. Within the fault zone, the local lithologies are usually extensively crushed and mixed; the low resistance of these fault rocks to subaerial erosion seems to be largely responsible for the 'rift morphology' along the trace of the transform. This rift morphology extends from Karliova to Mudurnu with only two minor interruptions by the pull-apart basins of Erzincan and Resadiye and finally merges with the horst and graben regime of W Anatolia, W of Mudurnu.

Attempts to estimate the age, throw and offset of the NATF have been mostly speculative. Ketin (1948) remarked that the feature is young, but did not propose a time of initiation. Pavoni (1961a) thought that the fault may have originated in the Early Tertiary and estimated its offset to be of the order of 350–400 km. Large amounts of field data have accumulated during the last 20 years to show that neither the age nor the offset along the fault is as great as Pavoni initially believed. Erinc (1973) pointed out that the original drainage network around the NATF was established during the Late Miocene, since when it has been modified by activity on the transform and a new drainage system, in places following the trace of the crushed zone for considerable distances, has been formed. Ketin (1976) pointed out that, within the rift zone, no sediments older than Middle Miocene have been found, indicating that at least the morphological expression of the fault did not exist prior to this time. Just W of Erzincan, Tatar (1975) mapped inactive branches of the NATF now covered by Pliocene sediments and concluded that the fault originated in pre-Pliocene times. Therefore, the geomorphological data constrain the origin of the fault to between late Early Miocene and Pliocene.

By detailed mapping around Resadiye, Seymen (1975) showed that the ophiolitic suture between the Pontide and Anatolide regimes is cut and offset by the transform. In this area, the major overthrusting of the Pontides onto the Anatolides took place during the Burdigalian and Seymen (1975) interpreted this as the manifestation of the terminal suturing between the two tectonic provinces, therefore arguing that the NATF must be of post-Burdigalian age in the segment between Amasya and Erzincan.

The apparent offset of the Pontide–Anatolide Suture between Amasya and Erzincan is about 85 km and Bergougnan's (1976) mapping revealed a similar offset. Seymen (1975) argues that, because the dip of the offset suture near the fault zone is sufficiently steep and the vertical motions along the fault zone are small compared with the horizontal component of movement, the apparent offset closely approximates the real offset. Several other lines of indirect evidence suggest an offset of the order of 80–100 km and an average rate of motion along the fault of 1–2 cm yr^{-1} (Canitez 1973; Arpat & Saroglu 1972). Tokay (1973) and Tatar (1975), provided several constraints on the possible minimum and/or maximum amounts of offset that bracket the cumulative offset between 50 and 100 km. Although a Quaternary rate of 9 mm yr^{-1} along the western, E–W, segment of the NATF is close to the 8.9 mm yr^{-1} average rate deduced for the eastern NW-SE segment, the total post-Tortonian slip on the western segment is only 25 km (Barka & Hancock 1984) compared with a total post-Serravallian 85 km on the eastern segment. Thus, some of the remaining 55 km of right-lateral motion can be accounted for by displacement that occurred before the latest Tortonian while some may have been taken up on other faults. Possibly either or both the Kure (Bergougnan *et al.* 1978) and Sungurlu Faults took up the motion, or the Kure Fault was a precursor to the western segment of the NATF, or the latter was a left-lateral structure during pre-Pleistocene times (Hancock & Barka 1981) and formed the southern boundary to a W-moving wedge similar to, but smaller than, the present Anatolian Block (Hempton 1982).

The large scale tectonics of Anatolia and surrounding regions does not support the idea of a large (more than a couple of 100 km) offset along the N Anatolian Transform Fault. Anatolian tectonic zones are traceable into the Hellenides (Bernoulli *et al.* 1974) and there is neither enough deformation in, nor enough room between, Anatolia and Greece to accommodate an offset more than 300 km along the NATF. On the other hand, a smaller offset, in the order of 80–100 km, would be compatible with the known geology and post-Oligocene tectonics of the Aegean area (Dewey & Şengör 1979). An even smaller offset of about 15 km along the EATF (Arpat & Saroglu 1972) supports this view. Further detailed geological mapping of, and synthesis of data on, the NATF is needed to establish the cumulative offset of the fault along various segments, to determine whether the offset changes in any way along the fault and whether the fault is composed of different segments that formed at different times and in response to different strain systems, as maintained by Ricou *et al.* (1975).

The NATF seems to have episodes of seismic unrest, separated in time by quiescent periods of about 150 yr (Ambraseys 1970). The most recent phase began with the 1939 Erzincan earthquake. A series of large earthquakes followed and outlined a general migration of seismic activity from E to W along the fault, a peculiar characteristic, first noted by Ketin (1948). During this last cycle of seismic activity, the style of seismicity of the NATF has been similar to the behaviour of the San Jacinto segment of the San Andreas Fault in California, characterized by frequent shocks with magnitude $6 < M < 7$ (Scholz 1977). Scholz (1977) argued that this type of behaviour characterizes those segments of large strike-slip faults that strike parallel with the regional slip vector between two plates, resulting in low normal stresses across the fault plane. This is approximately the case for the NATF, particularly for its well-defined, nearly pure strike-slip segment between Mudurnu and Karliova, if one uses McKenzie's (1972b) Anatolia/Black Sea pole of rotation located at lat. 18.8°N and long. 35°E.

Using the earthquake data for 1960–71, Alptekin (1978) computed the magnitude frequency relations for the NATF, and other seismic provinces in Turkey. He found b values of 0.73, 0.56 and 0.66 for western, central and eastern sections of the NATF, respectively. Alptekin (1978) considered the relatively low b-values found for the NATF as an indication of high strain accumulation, particularly in the central section of the fault. Seismic risk estimates based on magnitude frequency relations obtained by Alptekin (1978) appear to be highest (68% for $M > 8.0$, and for a time period of 100 yr) for the central section of the fault. In contrast with the NATF, Alptekin (1978) obtained a much higher b value (0.87) for the EATF.

Using fault lengths and average dislocations observed in the field, Canitez & Ezen (1973) derived a total seismic moment for the period 1900–71 of 1.77×10^{28} dyne cm. Using this value and following Brune (1968), they calculated the average slip rate for the period of interest for different fault depth assumptions. They found, for instance, 2.4 cm yr^{-1} for d = 20 km, 1.6 cm yr^{-1} for d = 30 km, and 1.2 cm yr^{-1} for d = 40 km. Stress drops for some earthquakes on the NATF have been investigated by Chinnery (1969) and Hanks & Wyss (1972). Canitez & Ezen (1973) concluded that the stress drop on the NATF is between 10 and 15 bar for $M > 7$ and does not depend on magnitude as expressed by Aki (1972). For $M < 7$, however, they found the stress drop to be less than 10 bar.

Fault plane solutions of earthquakes along the NATF have been presented mainly by Canitez & Ucer (1967a,b), McKenzie (1972b), Dewey (1976) and Jackson & McKenzie (1983). These solutions give consistently dextral slip with minor thrust components between about Eskipazar and Karliova. Because all major shocks produced surface breaks, there is no nodal plane ambiguity. East of Karliova, strike-slip movement continues on a line on strike with the NATF (Ambraseys & Zatopek 1968; Ketin 1969), but the fault plane solutions here indicate an increased amount of thrust component (Mckenzie 1972b), consistent with the left-lateral EATF (Arpat & Saroglu 1972; Seymen & Aydin 1972; McKenzie 1976) joining the NATF thus imposing a thrust component onto the segments E of Karliova. Strike-slip faults E of Karliova are elements of the convergent regime of the Turkish–Iranian Plateau (Şengör & Kidd 1979) and not continuations of the NATF. Strike-slip motion on these faults is due to their oblique orientation with respect to the Arabia/Eurasia convergence.

To supplement observations in the fields of seismology and geomorphology, high-precision triangulation and trilateration measurements were started by the MTA in 1972, in the western sector of the NATF (Gerede–Cerkes region). Comparison of the 1946 and 1972 measurements showed a 75 cm horizontal displacement along the eastern end of the 1944 Gerede–Bolu earthquake fault. The total relative displacement in the western portion, however, was 20 cm for the same period (Ugur 1974). Ambraseys (1970) reported an average displacement of 90 cm for the entire fault since 1939.

East Anatolian Transform Fault (EATF)

The seismically active and morphologically distinct EATF extends for 400 km from Karliova in the E to Maras in the W and marks the southeastern left-lateral, strike-slip boundary between the Anatolian 'Block' and the Syrian Foreland (McKenzie 1976). A Middle Miocene marker horizon near Golbasi and an unconformity between Miocene and crystalline rocks near Goynuk, are offset in a sinistral sense for 18 and 22 km respectively, and the Euphrates River for 15 km SW of Lake Hazar. Fault-controlled basins along the transform contain Pliocene lignite, bracketing the initiation of the fault between the medial Miocene and the Pliocene. The fault ends in two continental triple junctions where incompatibility has led to the formation of complex intracontinental basins (Karliova and Adana). Northwest-trending left-lateral, strike-slip faults splay from the main trunk (e.g. the Elbistan Fault) and become part of the internal Anatolian regime. Along the fault there is a major locking segment near Bingol, a site of frequent earthquakes (e.g. 22 May 1971), and at Celikhan.

The best exposures of the EATF are in the Goynuk River gorge near Choban Tasha, about 40 km NE of Bingol. The fault occurs within a narrow (about 0.25 km) zone of brecciation and shutter ridge (Allen 1965) topography. Palaeozoic marble is juxtaposed along vertical shear zones against Miocene–Pliocene basalt. A few exposures of basalt show narrow (approximately 15 cm), sharp zones of cataclasis where phacoidal or trapezoidal clasts are aligned with their long axes parallel with the shear zone, with a structural fabric defined by the clasts.

The Neogene sedimentary basin near Boran, which is economically important because of lignite deposits associated with the dominantly lacustrine sediments, appears to have been structurally controlled by the EATF. The Boran Basin is strongly deformed, mainly by faulting and, in its wider extents (as much as 5 km), shows spectacular strike-slip valley morphology. Angular fault blocks dissected by stream valleys, are tilted in all directions, a feature typical of strike-slip zones. Near Boran, a minor thrust fault is localized on a lignite bed originally perhaps 1 m thick. The lignite is converted to anthracite and high-grade bituminous coal and occurs in discontinuous lenses in which phacoidal cleavage and asymmetric folds determine the sense of offset in the lignite. Elsewhere in the Boran Basin, small thrusts of minor offset are indicated by conjugate fractures and Riedel shear assemblages. Between Bingol and Karliova, Recent gravel talus fans have no adjacent source and are clearly displaced from their original hillside sources by strands of the EATF. Several exposures show these gravels vertically shingled and deformed by cataclasis with underlying basement rocks. Probably, gravels slipped into extensional fissures in the basement along the fault and the fissures then closed and were deformed by transcurrent cataclasis. Barka & Hancock (in press) have demonstrated an identical origin for deformed gravels along the NATF.

Detailed mapping in the Lake Hazar area has revealed a 6 km wide fault zone composed of subparallel strike-slip, oblique-slip and normal faults surrounding a young pull-apart basin (Hempton 1980). Fault zone structure and morphology is very well exposed and uplifted lacustrine sediments contain deformed horizons, possibly seismites triggered by seismic activity (Hempton & Dewey 1983; Hempton *et al.* 1983).

Along the SW margin of Lake Hazar, fresh scarps cut basement rocks, transpose displaced segments of hill sides and dextrally offset streams and small delta fans. West of Lake Hazar, subparallel strike-slip and normal faults result in a 6 km wide asymmetric transform valley with a stepped southern wall. Strike-slip faulting dominates but parallel normal faulting occurs on the higher southern wall as fault blocks descend into the eroded transform valley.

The NATF and EATF join in a complex depression, the Karliova Basin, a Pliocene–Quaternary intermontane sedimentary basin approximately 1750 m ASL. The Quaternary surface of the basin is almost perfectly flat, yet no drainage larger than small juvenile streams flows through the basin. Coarse clastic sediments are limited to alluvial fans at the mouths of intermittent streams near the basin margin. None of the major faults (NATF, EATF, Varto) enter the basin as single strands, but occur as diffuse zones of brittle deformation. The arrowhead-shaped Karliova Basin appears to be a compatibility structure, a zone of extension caused by the westward motion of the Anatolian Wedge, with respect to the EACZ.

Geometrically, the Karliova Basin occupies an FFT triple junction (McKenzie & Morgan 1969). That the triple junction is contained entirely within continental lithosphere greatly complicates its evolution. If we allow the EACZ to shorten by vertical plane strain and the Anatolian Block to move westward on the NATF and EATF, a gap develops at the junction. As 'holes' in the lithosphere cannot exist, either the crust will extend by plastic flow or by complex faulting to close the gap, or the gap will be filled by igneous rocks and be the locus of intense volcanic activity. The complex fault pattern around Karliova (Seymen & Aydin 1972) may be due to such a complication. Where complex intracontinental strike-slip faults are generated in convergent environments, as in Iran, Afghanistan and Central Asia, such triple-junction holes may be responsible for basin formation and basaltic volcanism.

Most earthquakes on the EATF (including the 1971 Bingol earthquake) and surface faults occur in the pronounced bend of the EATF around Bingol (Arpat & Saroglu 1972; Seymen & Aydin 1972), but fault traces aligned with the other straighter parts of the EATF, occur to the NW of Bingol, where sharp folding occurs in the Neogene volcanic rocks (Arpat & Saroglu 1972). Reconnaissance field work has shown this area to be characterized by many recent fault scarps and surficial strain indicators. It appears that a compressional bend near Bingol is being cut off by a straighter fault to the NW much as the compressional bend of the San Gabriel Fault was truncated by the straighter San Andreas Fault during the Pleistocene.

Examination of the earthquake distribution and topography near Golbasi suggests that this area may represent a seismic gap. Epicentres are absent for a distance of about 160 km between Maras and the Celikhan compressional segment S of Malatya, and fault traces are not distinct on Landsat images. We think it probable that this segment of the EATF is accumulating strain energy to be released in the near future as a shock sequence that will propagate southwestwards from Çelikhan.

Ambraseys (1971) has shown from historical records that both the NATF and EATF have been active during the period 100–1700 A.D. and, his time-distribution plots of damaging earthquakes suggest that movements along the NATF and EATF are diachronous. From 0–500 A.D., the NATF was active while the EATF was quiescent. From 500–1100 A.D., the EATF was active while the NATF was quiet. In 1100 A.D. the pattern was reversed. Over the last century, the NATF has been more active. This accounts for its greater coverage in the literature, especially after its spectacular migration of large earthquakes westward from 1939 to 1968 (Dewey 1976). However, there is unequivocal Quaternary evidence for movement on the EATF (Allen 1975; McKenzie 1976; Hempton 1980). Its recent quiescence and past history of active–quiescent interludes, suggest that it may presently be 'locked' and storing elastic strain energy. In the near future, it may be as active and dangerous as the NATF. This makes it a critical area for evaluating seismic potential and predicting the character of surface faulting and is underscored by the recent construction of large dams and plans for nuclear facilities. Three segments of the EATF are particularly significant for future study: (i) a compressional soon-to-break bend near Bingol, (ii) an extensional pull-apart sag partially occupied by Lake Hazar, and (iii) a seismic gap SW of Celikhan. Modern seismology has been applied to the Middle East for the last three decades. Historical records going back 2000 yr illustrate discrepancies with the instrumental record. Both these records are inadequate when considering the time scale involved in tectonic processes. For more significant evaluations of seismic potential a much longer record is needed. As Allen (1975) and Ambraseys (1978) have emphasized, the geological history of Late Quaternary faulting is a promising source of statistics on the frequency, location and character of surface faulting of large earthquake shocks. Ambraseys (1978) notes that almost all shallow earthquakes of magnitude equal to, or greater than, about 6.7 have been associated with surface faulting. This surface faulting has occurred along faults that have or could have been recognized prior to the earthquake. Thus, for a more thorough understanding of the number of large earthquake events, maximum expectable magnitude, amount of displacement per event and recurrence interval along the EATF, it seems imperative to study its Late Quaternary geologic history. The benefits of this approach have been demonstrated in important studies by Sims (1973, 1975), Wallace (1977, 1978), Sieh (1978) and Swan *et al.* (1980).

An additional potential source of much important data is the detailed mapping of surface faults in active fault zones. This is a relatively unexplored avenue of earthquake research. It is reasonable to assume that the character of surface faults (width, length, continuity, distribution, pattern, behaviour at depth, texture of fault rocks, etc.) may reveal much about their causative faulting and earthquake processes (Bonilla 1979; Sibson 1983) and seismic risk.

East Anatolian Convergent Zone (EACZ)

The EACZ is bounded to the S by a complicated southward-prograding and S-vergent system of shallow-dipping thrusts (Assyrides) involving thin sheets of basement (Bitlis and Poturge Massifs), ophiolites and ophiolitic wildflysch, and thick Tortonian flysch sequences (Lice Flysch). This thrust complex is at present moving southwards (Lice earthquake) over its foreland flexural basin (Selmo Molasse) with a peripheral bulge some 200 km from the thrust front (Fig. 8). Both the foreland basin and foreland platform sequence contain some S-vergent folds and thrusts. The northern part of the Selmo foreland basin is S-sloping and is being uplifted and dissected much like the molasse of the Swiss Plain today. The Assyride Thrust Belt is undergoing present day strong uplift as witnessed by the antecedent Euphrates Gorge that cuts through the Poturge Massif and leaves the truncated beds of intermittent streams stranded high on its walls. The foreland has several large basalt spreads, especially immediately SW of Diyarbakir, which, from the distribution of small conical volcanic centres, were erupted from approximately N–S fissures. These N–S fissures are part of a widespread array of N–S fissures and grabens and conjugate fractures throughout the Arabian Shield, that appear to have been caused by the Neogene collision between Arabia and Turkey/Iran. Analogous structures, trending NE, but not accompanied by volcanism, characterize the eastern part of the Arabian Platform, SW of the Zagros Front and have been interpreted also as products of Iranian/Arabian collision by Hancock *et al.* (1984).

North of the Assyride Thrust Belt, the E Anatolian Plateau has a variable and complicated pattern of deformation. Neotectonic fractures (Fig. 8) box the compass and many clearly rejuvenate older structures. However, there is a preponderance of N–S fractures, some of which control the positions of volcanoes (Nemrut), NE-trending left-lateral, strike-slip faults and NW-trending right-lateral, strike-slip faults. The calc-alkaline double-peaked strato-volcano of Mount Ararat lies in a complex pull-apart graben on a wide zone of dextral transcurrent motion. Parasitic cones associated with the large volcanoes of Eastern Anatolia show N–S (Nemrut) and NW (Ararat) trends (Fig. 11). Analysis of the topography indicates that all elongate basins in the EACZ overlie a strike-slip fault and that most of the elongate high areas are bounded by strike-slip faults. It seems certain that some of the intra-continental convergent strain is taken up along these faults although their role is probably minor compared to the NATF and EATF. East of long. 41°E, the strike-slip faults are closely spaced, shorter and enclose larger angles about N–S bisectors, suggesting that they may have experienced external and/or internal rotation.

Several regions (e.g. Keban) are seismically quiescent and topographically smooth with relatively little relief and less fracturing and may represent more rigid stronger flakes. The Munzur Mountain block appears to be a thrust-bounded horst. Thrust and fold zones are important E of long. 41°E where Neogene

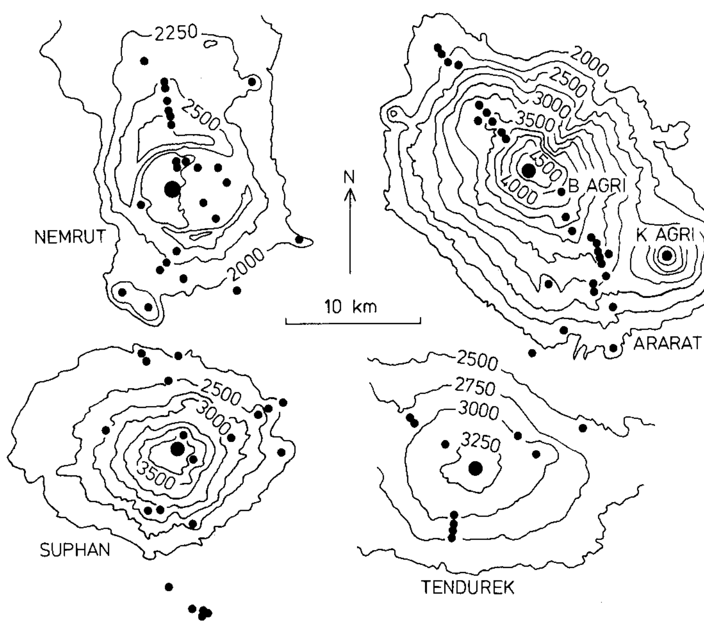

FIG. 11. Morphology of the four principal volcanoes of Eastern Anatolia contoured in metres and showing distribution of parasitic cones and small centres.

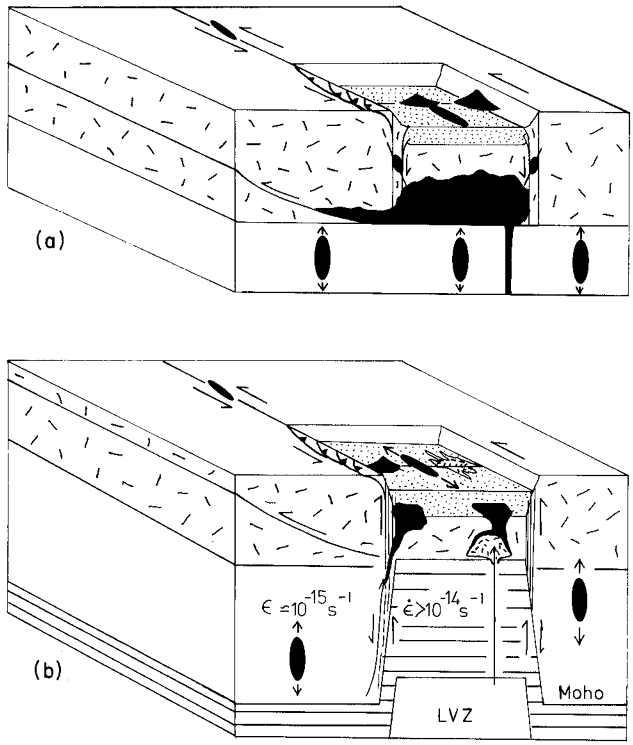

FIG. 12. Schematic strike-slip pull-apart basins involving (a) only the elastic lid (basement symbol), and (b) the whole lithosphere. Black: granite; fine stipple: sediment; fine random ornament: mafic igneous rocks of mantle origin.

basalts are strongly folded as, for example, along the northern margin of the Van–Mus Basin. Between these zones of strong folding the basalts are almost flat-lying, suggesting that strain-free regions (flakes) are bounded by zones of strong shortening (flake boundaries). The Upper Miocene basaltic andesites of the Solhan Formation (Fig. 10) show this variation particularly well, whereas the Pleistocene Holocene volcanics around Lake Van are almost unfolded. The Neogene volcanics of Eastern Anatolia hold great promise as strain guages for Anatolian deformation, for studies of both regional strain homogeneity and local and regional strain rate with time.

The fault, seismic, topographic and field data suggest a regionally inhomogeneous strain pattern in the EACZ. Crustal/lithospheric shortening appears to be accomplished by a complex interaction of horizontal plane strain by strike-slip wedge tectonics and vertical plane strain by the detachment of 10–15 km thick thrust flakes. The transpressional bend in the EATF at Celikhan coincides with the intersection with the Assyride thrust front and suggests that the precise location of the EATF is a flake boundary and coincides with a lithospheric transfrom only in a general way. Seismic activity, characterized by strike-slip and thrust slip, occurs around the fault bounded edges of the flakes within the upper seismogenic elastic layer. Faulting is probably discontinuous in space and time, accounting for the complex heterogeneous distribution of faults and seismic activity. East of long. 41°E, deformation has been more intense, where the lithosphere has probably suffered more bulk shortening and thickening than the region W of long. 41°E, where some shortening seems to be accommodated by slip along the NATF and EATF.

Basin development

Basins in Anatolia are of four types; the Selmo foreland flexural basin, pull-aparts on major strike-slip faults (Erzincan, Hazar), flake and plate triple-junction compatibility basins (Karliova and Adana) and elongate strike-slip/thrust-bounded basins (Van–Mus).

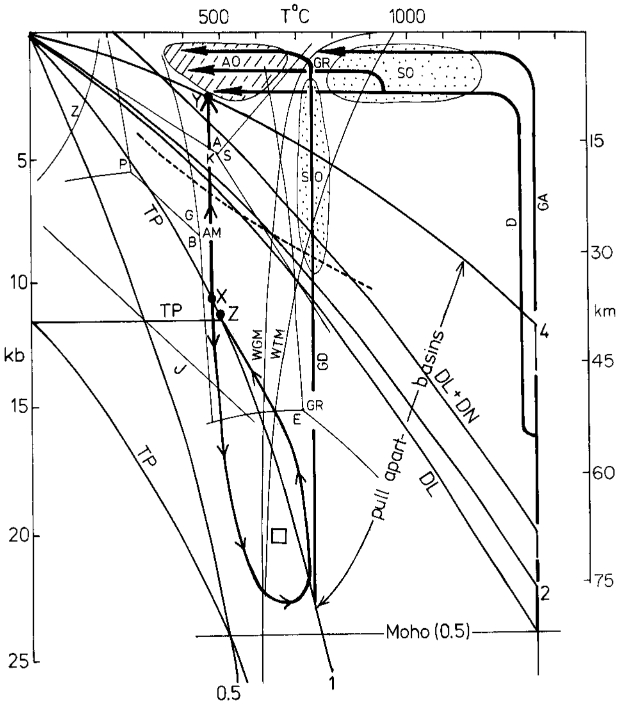

FIG. 13. Pressure/depth/temperature plot showing some possible relationships between the *P/T* paths of rocks in convergent orogens, associated igneous rocks and metamorphic facies. 0.5, 1, 2 and 4 refer to geothermal gradients appropriate to these heat flow values in HFU. Dotted line: geothermal gradient reconstructed for the Lepontine metamorphic core of the Alps (England 1978) at about 30 Ma; large square: kyanite eclogite in the Tauern fenster; DL, unrecovered geothermal gradient for crust delaminated at 65 km; DL + DN, unrecovered geothermal gradient for crust delaminated at 65 km and truncated by 5 km denudation; TP, unrecovered geothermal gradient for crust doubled by a single thrust *xy*: *P/T* paths of a point in a crust undergoing high strain rate, isothermal, horizontal stretching to $\beta = 4$. xz: *P/T* path of a point in a crust undergoing shortening by a value of 0.5 followed by denudational stripping. A, andalusite; AM, amphibolite; AO, andulusite overprint; B, blueschist; D, diorite; E, eclogite; GA, gabbro; G, greenschist; GD, granodiorite; GR, granulite; J, jadeite; K, kyanite; P, pumpellyite; S, sillimanite; SO, sillimanite overprint; Z, zeolite; WGM, beginning of wet granite melting; WTM, beginning of wet tholeiite melting (Yoder & Tilley 1962; Boettcher & Wyllie, 1968).

An interesting contrast exists between pull-apart basins on the NATF and those on the EATF. From the slip rates of the NATF and EATF and the lengths of pull-apart basins along them, the Erzincan Basin has an extensional strain rate of 10^{-13} s^{-1} while the Hazar Basin has one of 3.6×10^{-15} s^{-1}. Both pull-apart basins lie within the regionally thickened crust of Anatolia, yet the Erzincan Basin contains volcanics whereas the Hazar Basin does not. Strain rate may be the governing difference; in regions of high extensional strain rate the lithosphere may be thinning faster than it thickens by regional shortening and by thermal re-equilibration, thus allowing fertile mantle to depths where partial melting is possible (Figs 12b and 13). Alternatively, the Hazar Basin may be a pull-apart that affects only the elastic lid (Fig. 12a).

Shortening and thickening of the crust may be accomplished by either or both vertical stretching and thrust imbrication. Vertical stretching and thermal re-equilibration yields a *P/T* path of the general form $X \rightarrow Z$ (Fig. 13). Much higher geothermal gradients (Fig. 13) can be achieved by localized zones of rapid (isothermal) stretching, lithosphere delamination (Bird 1978; Houseman *et al* 1981) and very rapid uplift and denudation (England 1978; England & McKenzie 1982). Rapid Oligocene uplift and denudation was probably responsible for the Lepontine high *T/P* metamorphism in the Central Alps, whereas delamination and rapid lithospheric stretching in pull-aparts, also affords a rationale for mantle partial melting beneath and mafic igneous rocks in orogens (Fig. 13), perhaps accounting for the Ne/Hy normative basalts of Eastern Anatolia. Silicic but especially mafic melts are possible causes of both sillimanite and andalusite overprints of Buchan-type metamorphism (Fig. 13) and the position and shape of intrusions may be controlled by compatibility holes and gaps caused by flaking of the elastic lid particularly beneath pull-apart basins (Fig. 12). Rapid stretching of the lithosphere also affords an explanation for localized zones of andalusite-facies regional metamorphism not obviously related to intrusion. Isothermal stretching allows crustal rocks at appropriate levels to pass rapidly from sillimanite or kyanite fields into the andalusite field (Fig. 13, $X \rightarrow Y$). Thus, a spatial relationship is theoretically possible between pull-apart rift basins at high levels and andalusite growth and horizontal stretching fabrics at deeper levels.

The Mus–Van Basin is an elongate structure along the northern edge of the Bitlis Massif forming a sediment plain in the Mus region and the deeper parts of Lake Van. In Lake Van, reflection profiles show considerable but zonal fault-controlled sediment deformation, particularly in the northern part of the basin (Degens & Kurtman 1978). Similarly, along the northern margin of the Mus segment, Miocene carbonates and basalts are strongly folded and locally cleaved. The Mus segment has a southerly slope, which has controlled the progressive southward migration of the Murat River. Terraces along the Murat River, just N of the basin, slope southwards from 20 and 3 m to the Murat alluvial plain in a distance of some 5 km and artesian conditions exist in the basin. Pliocene/Pleistocene alluvial gravels and sands in the Mus segment are affected by small thrust, normal and wrench faults on a fairly penetrative scale. A seismic reflection profile kindly loaned by TPAO (Turkish Petroleum Company) shows that the Mus segment contains up to 4 km of Late Miocene to Pleistocene sediment along its northern margin but thinning and overlapping southwards. The northern margin appears to be a transform/thrust right-lateral flower structure (a structure in which a narrow zone of strike-slip displacement at depth widens or flowers upwards into a zone of *en échelon* thrusting) and the Mus–Van Basin may be regarded as a ramp/strike-slip basin along a flake margin. The volcanics of Nemrut appear to truncate the basin unconformably.

The Adana Basin is a lithospheric extension zone at the edge of the Anatolian Plateau. It could be a major pull-apart in a complex left-lateral transform zone that continues the EATF trend, but its position at the Africa/Syria/Anatolia triple junction (Fig. 14) offers a better kinematic explanation. A vector triangle derived from the known trends and slip rates of the EATF (1.7 mm yr^{-1}) and the Syrian segment of the Dead Sea Transform Zone (4 mm yr^{-1}) yields an Africa/Anatolia slip vector of 3.4 mm yr^{-1} (Fig. 15) which gives NNW extension in the Adana region close to the Maras triple junction. A normal fault first motion derived NW-trending slip vector, for an earthquake on the northern edge of the Adana Basin (Canitez & Ucer 1967), is close to this extensional azimuth. The Adana Basin may be, therefore, simply a compatibility gap resulting from the evolution of an FFF plate triple junction.

Balancing and the slip vector

We now consider possible relationships between shortening, crustal thickening, strike-slip faulting and relative plate motion. Figure 14 summarizes the tectonics of Eastern Anatolia, and Fig. 15 is a vector diagram that relates relative plate displacements, slip on the NATF and EATF, and strain in Eastern Anatolia. The average convergence slip rate between the Arabian and European Plates for the last 14 Ma has been 15.3 mu yr^{-1} giving an average strain rate of about 2.0×10^{-15} s^{-1} in the EACZ, the slip rate derived by adding the Dead Sea transform slip rate (AF/AR, 5.3) to the Europe/Africa slip rate (EU/AF, 10). This Europe/Arabia rate may be too high for Anatolia, because the average slip rate on the Dead Sea Transform, N of the Antilebanon, has been 4 mm yr^{-1}, suggesting motion between the Arabian and a smaller Syrian Plate across the Antilebanon/Palmyran Zone, a zone of present-day weak seismic activity and recent shortening (A. Quennell, pers. comm.). If a Europe/Syrian (EU/SY) convergence rate of 14 mm yr^{-1} is appropriate, the average E Anatolian strain rate is slightly reduced.

A Europe/Syria/Anatolia (ANX) vector triangle (Fig. 15) is constructed from the length and trend of the Europe/Syria slip and the trends of the NATF and EATF. This construction indicates that, were the Europe/Syria convergence taken up solely by lateral wedging of a rigid Anatolian Block, the slip rates on the NATF and EATF would be 18.5 mm yr^{-1} and 19.3 mm yr^{-1} respectively. An 85 km offset of a Miocene suture along the NATF (Şengör

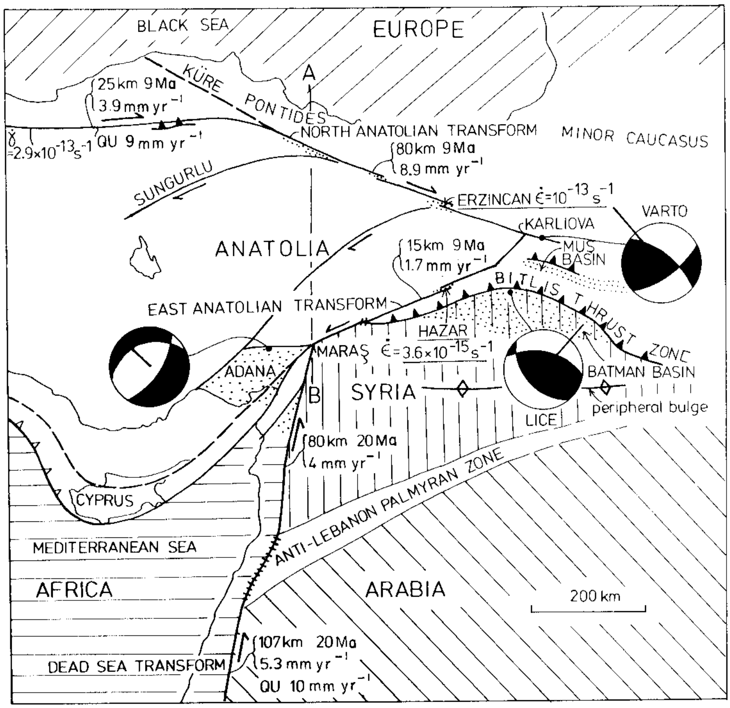

FIG. 14. Simplified tectonic map of Central and Eastern Anatolia and the Arabian Foreland showing slip rates on major faults, focal mechanisms for the Varto, Lice and Adana earthquakes (dilational quadrants: white; compressional quadrants: black, see also Fig. 9), young basins (stippled) and major plates (each with separate lined ornament) bounding the eastern plate boundary zone.

1979) gives a slip rate of 8.9 mm yr^{-1} and a 15 km offset of the antecedent Euphrates River a slip rate of 1.7 mm yr^{-1} along the EATF. Therefore, only a small part of the Europe/Syria convergent displacement is taken up by slip on the NATF and EATF. Slip on the NATF and EATF may be combined to give an approximation of the slip direction and rate on the Varto Fault, a steeply NE-dipping thrust immediately E of the Karliova junction; the coincidence with the slip direction derived from the fault plane solution for the Varto earthquake (Dewey 1976) is reasonably close. The portion of the EU/SY convergence vector that is not taken up by wedging and slip on the Varto Fault is given by the SY/SY join, which represents possible combinations of strain within the Anatolian Wedge between the NATF and EATF and strain between the Bitlis Thrust Zone and the Minor Caucasus. The SY/SY join is close in azimuth to the slip vector on the NE-dipping Lice Thrust derived from the fault plane solution for the Lice earthquake. The Europe/Syria convergence is taken up E of the Karliova junction by a complex array of southward-verging thrusts in the Bitlis Zone, several zones of folding and thrusting and NW-trending right-lateral faults. Thus, E of a N–S line AB (Fig. 14) through Maras, about a third of the convergence between Syria and Europe is taken up by wedging and westward slip of the Anatolian Block while the rest is accommodated by thrusting in the Bitlis Zone, folding and thrusting on other zones of shortening, displacement on mainly right-lateral, strike-slip faults and internal strain within the Anatolian Block.

West of line AB, convergent plate motion across the Anatolian Block is constrained by the Europe/Africa motion of 10 mm yr^{-1}; the AF/AN join of 10.5 mm yr^{-1} represents an unknown combination of slip on the Africa/Anatolian boundary and strain within the Anatolian Block. If no internal Anatolian strain is occurring, the AF/AN join gives the Africa/Anatolia slip direction.

That internal Anatolian Block strain has occurred both E and W of line AB, is shown by the 2 km high plateau which indicates a crust thickened to about 52 km, assuming

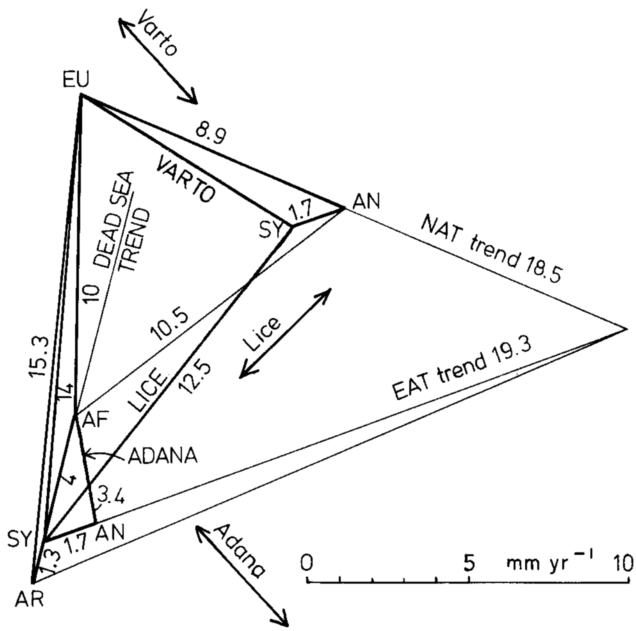

FIG. 15. Vector diagram for Eastern Anatolia. Slip rates in mm yr^{-1}. AF, Africa; AN, Anatolia; AR, Arabia; EAT, E Anatolian Transform Fault; EU, Europe; NAT, N Anatolian Transform Fault; SY, Syria.

approximate isostatic balance. Thus, in addition to convergence accommodated by strike-slip motion, which alone, can allow only a horizontal plane strain, the crustal thickening indicates about 80% vertical stretching. How this vertical component is structurally accommodated is unclear, as is its temporal relationship with strike-slip faulting. A similar tectonic situation exists in Tibet where a 5 km plateau caps an 80 km crust probably thickened by vertical stretching (Dewey & Burke 1973; England & McKenzie 1982).

Another approach to relating crustal thickening and lateral flow is to compare the cross-sectional input into the convergent zone from plate slip rates with the cross-sectional area present in the convergent zone (Fig. 16). For the Himalayas and Tibet, a convergence rate of 50 mm yr^{-1} for 40 Ma has contributed 6.2×10^4 km^2. We add this to the material originally in the 1000 km long box (3.1×10^4 km^2. About 20 km has been denuded from the High Himalayas, whereas the Tibetan Plateau has suffered little denudation except for perhaps as much as 5 km to expose granites along its southern border. This gives a maximum of 3.25×10^3 km lost by denudation; 7.755×10^4 km^2 is the cross-sectional area of crustal material in Tibet. The missing 1.22×10^4 km^2 must be accounted for by a combination of lateral flow from the section plane and perhaps by the thrust restacking of thinned crust in the Himalayas. A similar calculation for Eastern Anatolia (Fig. 16) yields the very small missing value of 12×10^2 km^2 according with the low slip rates on the NATF and EATF.

Plane strain shortening and vertical stretching of the crust, followed by lateral flow and spreading in the overall extent of the deformed zone once the crust has reached a thickness of about 80 km, has substantial implications for orogenic polyphase strain sequences and fabrics below the elastic lid and for fault sequences and tectonic regimes in the elastic lid (Fig. 17). With no denudation, constant volume and assuming coaxial bulk strain, vertical plane strain proceeds to 63% shortening, followed by a phase of horizontal plane strain at 168% bulk stretching that yields an oblate bulk strain at 86% shortening. Further shortening gives an oblate bulk strain at progressively higher K values. If an Argand value of 3 buffers crustal thickness at about 80 km, plane strain at shortening values greater than 63% may be accomplished where denudation accompanies shortening, where volume loss occurs, or by non-coaxial strains in high strain

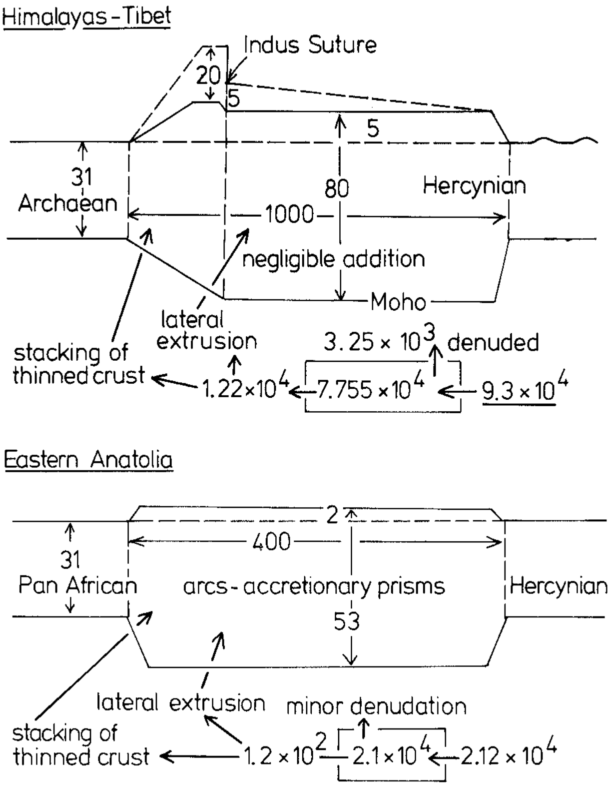

FIG. 16. Crustal balancing diagrams for the Himalayas/Tibet and Eastern Anatolia. Cross-sectional areas in km^2 and heights and lengths in km. Area fed in by convergent plate motion underlined. Area within deformed zone in box.

zones. This model predicts that lateral wedging along major strike-slip faults with their associated pull-apart basins will be superimposed on the orogen at a late stage and accounts well for the young N–S grabens of the Tibetan Plateau.

Conclusions

After initial contact, continent–continent convergence results in two phases of deformation (Dewey & Şengör 1979). Because of the irregular shapes of continental margins characterized by salients and embayments, collisional deformation begins at projection points of initial impingement, separated by oceanic embayments. Continued convergence results in thrusting and strike-slip movement of continental slivers over open boundaries of the remaining oceanic crust (McKenzie 1972b; Dewey & Burke 1973). Most of the convergent strain is confined to the zone defined by the extent of remaining oceanic lithosphere. When all the oceanic lithosphere in the system is eliminated, a much broader phase of bulk intra-continental shortening and thickening commences near the suture (e.g. Tibet), accompanied by more distant foreland deformation characterized by large intracontinental strike-slip faults laterally moving huge blocks of continental lithosphere (e.g. in Eastern Asia). In this phase, convergent strain is distributed up to thousand of km from the suture zone of initial collision.

Molnar & Tapponnier (1975, 1977a,b, 1978, 1979) have explained the pattern of large strike-slip faults in the Asian Foreland, comprising China, Mongolia and the southeastern U.S.S.R., as being analogous to slip lines developed experimentally in plastic materials when indented by a rigid die. This model for continental crustal deformation breaks down when considered in detail. Not all strain is distributed in uniformly spaced strike-slip faults. There is significant folding and thrusting in and around the Tien Shan, Nan Shan, and Lung Men Shan. Large areas of extension occur where strike-slip faults sidestep close to

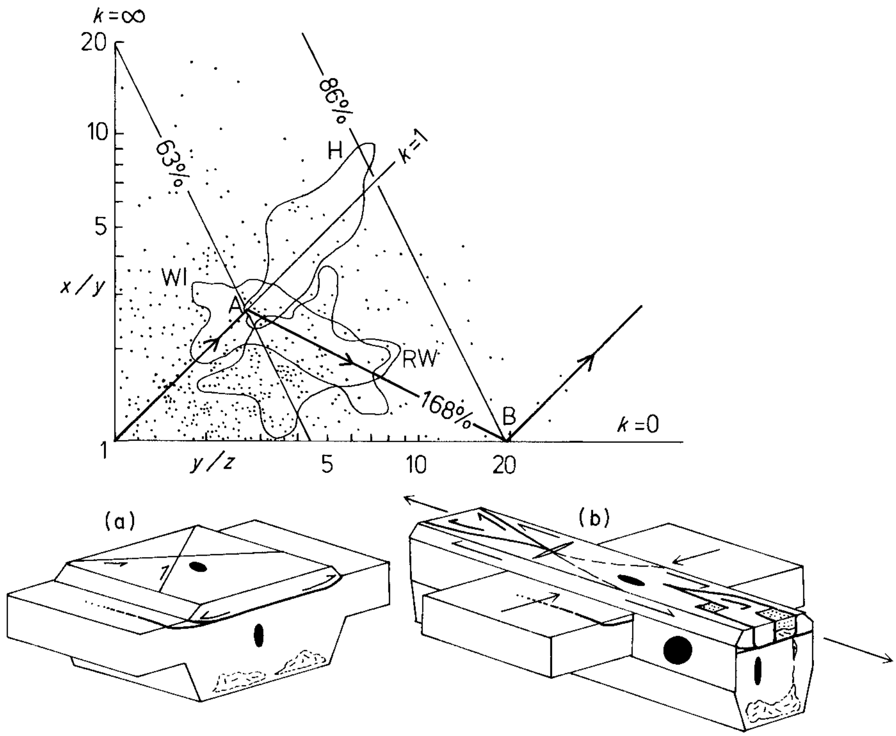

FIG. 17. Log deformation plot with shortening lines at 63 and 86% and elongation line at 168%. Arrowed line is theoretical strain path for a crust originally 31 km thick shortened by vertical plane strain and thickened to 80 km (a), followed by horizontal plane strain by lateral extrusion (b). Dots: strain states replotted from Pfiffner & Ramsay (1982). Enveloped areas: H, Dalradian slides (Hutton 1979); RW, slates (Ramsay & Wood 1976); WI, Palaeozoic rocks of western Ireland (Dewey 1969).

the 'open' oceanic boundary to the E as in the Baikal Rift System, the Shansi Graben System and the Yunnan Grabens. Movement on large foreland strike-slip faults is significant during orogeny and probably continues after superficial folding as shown by parallel post-folding strike-slip faults in the Hercynian of Northern Africa (Mattauer *et al.* 1972; Arthaud & Matte 1977) and the Proterozoic of the Canadian Shield. However, the motion of the Anatolian Wedge, with respect to its northern and southern neighbours and the movement of the bounding transform faults with respect to the bisector of their dihedral angle, resembles greatly the situation encountered in plastic extrusion in a modified Prandtl Cell. The faults that bound the Central Anatolian ovas are similar to the slip lines in the Prandtl Cell. Similar models of plastic behaviour have been proposed to explain large-scale fault patterns in the Mojave Desert of California (Cummings 1976) and in the Caribbean (Burke *et al.* 1978). Such comparisons should be approached cautiously; the models apply only to two-dimensional instantaneous patterns whereas the geological structures with which they are compared are three-dimensional objects evolving over millions of years. The pattern comparison should be made only where the detailed geological picture is known; this is not yet the case for Anatolia.

It is suggested the there is a causal relationship between the NATF, EATF and the extensional ova regime of Central Anatolia. This provides a possible and testable solution to the geometrical as well as temporal aspects of the longstanding ova problem in Anatolia. Similar pairs of large-scale strike-slip faults exist elsewhere in continental lithosphere; in the Mojave Desert of California, their possible role in controlling the deformation of continental lithosphere was noted by Cummings (1976). More detailed field evidence will have to be obtained, especially to discover whether or not there is any systematic change in the amount of offset along the NATF and

EATF and to determine the precise geometry of the Karliova triple junction and the fault system that formed the Anatolian ovas and the age and subsidence history of the ovas. Microearthquake surveys within Anatolia may provide further information as to whether or not the deformation in the Anatolia Wedge, which appears from Quaternary geology to be active, is generally free of earthquakes and is thus perhaps proceeding in a non-brittle fashion.

Slip-line field theory may be appropriate for describing deformation below the brittle seismogenic zone associated with large strike-slip faults (Earton *et al.* 1970; Ben-Menahem 1976). Recent fault zone models consider strain to be accommodated via creep, in zones that deform plastically (Prescott & Nur 1981). Differences in the pattern of large strike-slip faults in Eastern Asia and experimental patterns of slip lines may be due to crustal heterogeneity as well as different boundary conditions. Perhaps we should consider upper-crustal convergent deformation in terms of domains or flakes of ductility contrast at all scales. Older crustal domains are cooler and thicker (Sclater & Francheteau 1970) and therefore stronger than younger, hotter and weaker crustal domains. This is particularly well developed in Eastern Asia (Molnar & Tapponnier 1981). The Precambrian shields, India, Tarim and Angara, are relatively undeformed and have been little affected by the India–Eurasia convergence since the Tertiary. Conversely, the Mesozoic and Tertiary terrane of Tibet has suffered extensive diffusely distributed deformation (Landsat imagery studies by J.F.D. and W.S.F.K.). Palaeozoic terranes of Tien Shan, Altai and Khangal are deformed but in a less diffuse style than in Tibet. A ductility contrast probably also explains the less deformed nature of the Lut Block in Iran (Mohajer-Ashjai *et al.* 1975).

Many factors affect the structural style and tectonics of continental collision zones, such as their width, amount of shortening, the role of lateral wedging, the extent to which plateaux are developed and degree of strike continuity, among many others. We list and outline below those factors that we believe are important in determining collisional orogenic style and which, in combination, determined the great range of styles and geometries in the Alpine/Himalayan system (Fig. 1).

First, the amount, rate, style, duration and timing of lithospheric stretching that generated the continental margins and rifts involved in subsequent collision-induced shortening may vary considerably. Where large β values occurred — up to a maximum of about 4.5, Dewey (1982) — the mantle is brought near the surface and is more likely to be involved in subsequent flake detachment. The width over which stretching occurred may vary from very narrow, as for the sharply defined Red Sea margins, to over 100 km, as for the more diffuse Bay of Biscay margin. Hence, subsequent collisional margins will correspondingly vary from the sudden impingement of sharp ramparts to the more progressive restacking of thicker and thicker crust along listric faults that cut progressively deeper into the thickening crust. The polarity of earlier listric normal faults appears, generally, to be 'down to ocean or rift' so that thrust regeneration induces a continent-ward thrust polarity. However, reversed polarity arrays of normal faults occur for example in the Gulf of Suez, separated from normal polarity arrays by transform relays. Thrust remobilization of such arrays would generate early *rétrocharriage* basement nappes. The time elapsed between stretching and subsequent shortening determines the thermal age of the continental margins, i.e. its lithospheric thickness, geothermal gradient, strength profile and hence, the thickeness of the elastic lid and position of detachment zones during collision. Thermally young *v.* old margins will have thin *v.* thick thrust flakes respectively.

A second factor is the nature and history of the colliding crust. If the collisional zone results from the collapse and inversion of ultrarifts (Alps), collisional, thrust stacking occurs from the beginning of convergence. Orogens with substantial strike continuity result, although individual basement nappes may be laterally impersistent. Where collisional zones are the terminal culmination of a longer history of oceanic closure, often of several oceans (Himalayas/Tibet), continental margins may consist of assemblages of collided and laterally transposed blocks, arcs, exotic terranes and subduction-accretion prisms (Coney *et al.* 1980), along whose boundaries tectonic mobilization can occur during collision. Furthermore, a long subduction history will thermally weaken the overriding margin and render it more susceptible to convergent deformation. The time since earlier stabilization of colliding cratons — i.e. their thermal age — plays a fundamental role not only in determining the amplitude and wavelength of foreland flexures (Karner & Watts 1983), but also in the extent and style of foreland/hinterland deformation. The Archaean shield of

India is little affected by collisionally-induced deformation whereas the younger more inhomogeneous Sinian hinterland is affected by thickening, wedging, folding and rifting for several thousand km from the Tsangpo Suture. Continental crust varies greatly in character from the anhydrous granulitic terrains, typical of some Proterozoic orogens, to hydrous subduction accretion prisms (Dewey & Windley 1981). The consequent lateral and vertical variations in bulk rheology of crustal profiles and the positions of potential detachment surfaces, determined both by the brittle–ductile transition and by crustal inhomogenities, controlled stratigraphically and petrographically (Fig. 5), will be important in determining strains and displacements during collision.

Thirdly, collisional geometry and history is controlled to a large extent by the shapes of colliding margins. Continental margins vary from rather simple and straight (Chile) to complex and irregular with promontories and embayments. Therefore, collision is likely to be diachronous from promontories, from which lateral crustal flow and wedging occurs, to embayments that subduct beneath lateral wedges, which may expand above subduction zones (Aegean), and receive the erosional products of the colliding promontories and close last. Hence great lateral variations may be induced in collisional orogens (Dewey & Burke 1973; Dewey & Kidd 1974).

Fourthly, the direction, rate, duration and degree of convergence are a controlling influence. Very oblique convergence induces a strong strike-slip component (Dewey & Shackleton 1984). A high convergence rate feeds continental lithosphere into the convergent system at high rates, which in turn may generate a wider orogen (Ben-Avraham & Nur, 1976). Average strain rates appear to be remarkably constant at about $1.5 \times 10^{-15}\ s^{-1}$, which indicates a buffering mechanism, probably olivine flow laws (England 1983). The duration of post-collisional convergence probably results from the configuration and evolution of the other boundaries of the plates involved in the collisional zone (Bott 1982; Bott & Kusznir 1984). Where a long period of convergence occurs, shortening zones appear to become wider (England & McKenzie 1982) and large amounts of shortening may impose a strong cylindroidism on the orogen.

Fifthly, the age of collision may be important. Average plate thickness and slip rate has decreased with time (Dewey & Windley 1981). This is reflected in considerable differences between earlier Precambrian and later Phanerozoic orogens. Precambrian deformation zones are wider with shorter wavelength flexural features, pervasive fore-

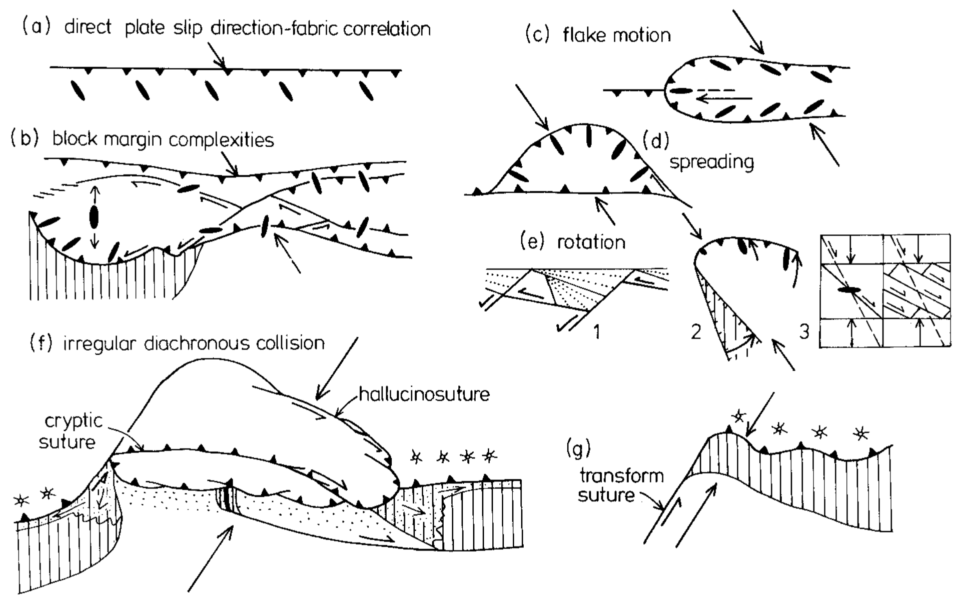

FIG. 18. Relationships between plate boundary slip vectors faulting and fabrics. Discussion in text. Oceanic lithosphere indicated by vertical lines, black ellipses: schematic sections through strain ellipsoids. All plan view except e1 which is a section.

land deformation and thicker stratigraphic sequences.

Displacement and strain within the whole plate boundary zone should integrate to equal the slip vector between the converging plates. The strain continuum or strain/displacement homogeneity problem is of fundamental importance to the basic and difficult question of the relationship between plate tectonics and classical structural geology, i.e. the extent to which, and under what conditions, relative plate slip vectors are directly expressed in structural geometry and fabric and, critically, how plate slip vectors can be deduced from integrated structural studies. Along narrow and well-defined oceanic plate boundaries, a fairly direct and relatively simple relationship between slip vector and structure might be expected at, for example, ridge/transform systems in subduction-accretion prisms and along ophiolite obduction zones. Perhaps a simple relationship (Fig. 18a) would be expected also where the first feathering collisional contacts are made by thrust restacking in zones of thin continental crust below sea level and commonly in the blueschist facies (Dewey, 1982), where body forces are not yet important. As collisional tightening and crustal thickening proceed, complexities increase, particularly in the elastic lid, by the complex motions of crustal flakes (Fig. 18b) much of which are induced by diachronous irregular collision and controlled by older crustal boundaries and other inhomogeneities (Fig. 18f).The earlier simpler relationship between structure and slip vector progressively breaks down. Flakes and blocks at many scales rotate about both horizontal (Fig. 18e1) and vertical (Fig. 18e2) axes inducing great local variations in strain axes and causing the reorientation of early formed structures by both internal and external rotation (Fig. 18e3). The lateral wedging of flakes (Fig. 18c) causes great variations in slip direction at their margins and the lateral flow of blocks over oceanic tracts (Fig. 18b) may cause (Aegean) extension in the overall plate convergence direction. Lastly, gravity spreading from zones of thickened to unthickened crust will generate structures that may bear little relationship to the plate slip direction.

If relationships are to be established between structure and plate slip vector therefore, we should be concentrating probably on ophiolite obduction aureoles and the earliest high strain zones in the blueschist facies. Later flaking may rotate many of these earlier formed structures but systematic palaeomagnetic work will be an important tool in discovering and sorting out these possible rotations.

Of course the recognition and understanding of continental collision depends upon our ability to recognize and understand collisional sutures, whose position is not always readily apparent. Sutures may be exceedingly cryptic (Dewey & Burke 1973). Also oceans may close along one boundary by transform motion (Fig. 18g) which drags in slivers of oceanic lithosphere along a transcurrent fault zone. As Robert Shackleton once remarked, 'a cryptic suture is one that exists and you can't see but a hallucinosuture [Fig. 18f] is one that you think you can see but doesn't exist'.

ACKNOWLEDGMENTS: We are deeply indebted to Paul Hancock and John Platt who greatly improved an early draft of this paper.

References

ADAMIA, S. A., LORDKIPANIDZE, M. B. & ZAKARIADZE, G. S. 1977. Evolution of an active continental margin as exemplified by the Alpine history of the Caucasus. *Tectonophysics*, **40**, 183–99.

AKI, K. 1972. Earthquake mechanisms. *Tectonophysics*, **13**, 423–46.

ALLEN, C. R. 1965. Transcurrent faults in continental areas. *Phil. Trans. R. Soc. London*, **A258**, 82–9.

—— 1969. Active faulting in northern Turkey. *Contr. No. 1577, Div. Geol. Sci., California Institute of Technology*, Pasadena.

—— 1975. Geological criteria for evaluating seismicity. *Bull. geol. Soc. Am.* **86**, 1041–57.

ALPTEKIN, O. 1978. Magnitude-frequency relations and deformation release for earthquakes that occurred in Turkey and its vicinity. *Contr. No. 6, Karadeniz Teknik Univ., Dept Geophys.*, Trabzon, Turkey.

AMBRASEYS, N. N. 1970. Some characteristic features of the North Anatolian Fault Zone. *Tectonophysics*, **9**, 143–65.

—— 1971. Value of historical records of earthquakes. *Nature, Lond.* **232**, 379–97.

—— 1978. Middle East — a reappraisal of the seismicity. *Q. Jl Engineering Geol.* **11**, 19–32.

—— & ZATOPEK, A. 1968. The Varto Ustukran (Anatolia) earthquake of 1966 August 19: a summary of a field report. *Bull. Seism. Soc. Am.* **58**, 47–102.

ARGAND, E. 1924. La tectonique de l'Asie. *Rep. 13th Int. Geol. Congr.* **1**, 171–372.

ARMBRUSTER, J., SEEBER, L., & JACOB, K. H. 1978.

The northern termination of the Himalayan mountain front: active tectonics from microearthquakes. *J. geophys. Res.* **83**, 269–82.

ARPAT, E. & IZ, H. B. 1977. 1976 Caldiran Depremi. *Yeryuvari ve Insan*, **2**, 29–41.

—— & SAROGLU, F. 1972. The East Anatolian Fault System: thoughts on its development. *Bull. miner. Res. Explor. Inst. Ankara*, **78**, 33–9.

ARTHAUD, F. & MATTE, P. 1977. Late Paleozoic strike-slip faulting in southern Europe and northern Africa: result of a right-lateral shear zone between the Appalachians and the Urals. *Bull. geol. Soc. Am.* **88**, 1305–20.

ATAMAN, G., BUKET, E. & CAPAN, U. Z. 1975. Could the North Anatolian Fault Zone be a palaeo-Benioff Zone? *Bull. miner. Res. Explor. Inst. Ankara*, **84**, 97–102.

BARAZANGI, M. & NI, J. 1982. Velocities and propagation characteristics of P_n and S_n beneath the Himalayan arc and Tibetan plateau: possible evidence for underthrusting of Indian continental lithosphere beneath Tibet. *Geology*, **10**, 179–85.

BARKA, A. A. & HANCOCK, P. L. 1984. Neotectonic deformation patterns in the convex-northwards arc of the North Anatolian Fault Zone. *In*: DIXON, J. E. & ROBERTSON, A. H. F. (eds) *The Geological Evolution of the Eastern Mediterranean.* Spec. Publ. geol. Soc. London, pp. 763–74. Blackwell Scientific Publications, Oxford.

BARTON, C. M. & ENGLAND, P. C. 1979. Shear heating at the Olympus (Greece) thrust and the deformation properties of carbonate at geological strain rates. *Bull geol. Soc. Am.* **90**, 483–92.

BECK, M. E. 1976. Discordant palaeomagnetic pole positions as evidence of regional shear in the western Cordillera of North America. *Am. J. Sci.* **276**, 694–703.

BEIN, A. & GVIRTZMAN, G. 1977. A Mesozoic fossil edge of the Arabian plate along the Levant coastline and its bearing on the evolution of the eastern Mediterranean. *In:* BIJU-DUVAL, B. & MONTADERT, L. (eds) *Structural History of the Mediterranean Basins*, pp. 95–110. Editions Technip, Paris.

BEN-AVRAHAM, A. & NUR, A. 1976. Slip rates and morphology of continental collision belts. *Geology*, **4**, 661–4.

BEN-MENAHEM, A. 1976. Tectonics, seismicity and structure of the Afro–Eurasian junction — the breaking of an incoherent plate. *Physics earth Planet. Interiors*, **12**, 1–50.

BERBERIAN, M. 1976. Seismotectonic map of Iran, scale 1/2,500,000. *In*: BERBERIAN, J. (ed.) *Contribution to the Seismotectonics of Iran. II. Iran Geol. Surv. Rep.* **39**, 516 pp.

BERGOUGNAN, H. 1976. Structure de la Chaine pontique dans le Haut-Kelkit (Nord-Est de l'Anatolie). *Bull. Soc. géol. France*, **18**, 675–86.

——, FOURAUIN, C. & RICOU, L. 1978. Les deux troncons et le double jeu de la faille nord-anatolienne. *C.r. Acad. Sci., Paris*, **287**, 1183–6.

BERNOULLI, D., DE GRACIANSKY, P. C. & MONOD, O. 1974. The extension of the Lycian Nappes (SW Turkey) into the southeastern Aegean islands. *Eclog. geol. Helv.* **67**, 39–90.

BIRD, P. 1978. Initiation of intracontinental subduction in the Himalaya. *J. geophys. Res.* **83**, 4975–87.

BLUMENTHAL, M. M. 1945a. Ladik deprem batti. *MTA Mecmuasi*, **1/33**, 153–74.

—— 1954b. Die Kelkit-Dislokation und ihre tektonische Rolle. *MTA Mecmuasi*, **2/34**, 372–86.

BOETTCHER, A. L. & WYLLIE, P. J. 1968. Melting of granite with excess water to 30 kilobars pressures. *J. Geol.* **76**, 235–44.

BONILLA, M. G. 1979. Historic surface faulting–map patterns, relation to subsurface faulting, and relation to pre-existing faults. *In: Proceedings of Conference VIII: Analysis of Actual Fault Zones in Bedrock, Open File Rep.* **79–1239**, 36–65, U.S. Geological Survey, Menlo Park, California, U.S.A.

BOTT, M. H. P. 1982. Origin of the lithospheric tension causing sedimentary basins. *Phil. Trans. R. Soc. London*, **A305**, 319–24.

—— & KUSZNIR, N. J. 1984. The origin of tectonic stress in the lithosphere. *Tectonophysics*, **105**, 1–13.

BRINKMANN, R. 1976. *Geology of Turkey*, 158 pp. Ferdinand Enke, Stuttgart.

BRUNE, J. N. M. 1968. Seismic moment, seismicity and rate of slip along major fault zones. *J. geophys. Res.* **73**, 777–84.

BRUNN, J. H., DUMONT, J. F., DE GRACIANSKY, P. C., GUTNIC, M., JUTEAU, T., MARCOUX, J., MONOD, O. & POISSON, A. 1971. Outline of the geology of the western Taurids. *In:* CAMPBELL, A. S. (ed.) *Geology and History of Turkey*, pp. 225–55. Petrological Exploration Society, Libya, Tripoli.

BONCEV, E. 1974. Generalities of the Kraistide–Vardaride Lineament. *In*: MAHEL, M. (ed.) *Tectonics of the Carpathian Balkan Regions*, pp. 330–2. Dionyz Stur, Bratislava.

BURKE, K., FOX, P. J. & SENGOR, A. M. C. 1978. Buoyant ocean floor and the evolution of the Caribbean. *J. geophys. Res.* **83**, 3949–54.

BUYUKASIKOGLU, S. 1979. *Seismolojik Verilere Gore Guney Anadolu ve Dogu Akdenizde Avrasya-Afrika Leuha Sinirinin Ozellikleri*, 75 pp. Istanbul Technical University, Istanbul.

BYERLEE, J. D. 1968. Brittle–ductile transition in rocks. *J. geophys. Res.* **73**, 4741–50.

CANITEZ, N. 1962. Gravite ve sismolojiye gore Kuzey Anadoluda Arz kabugunun yapisi. *ITU Maden Fak. Yay., Istanbul*, 87 pp.

—— 1973. Yeni Kabuk hareketlarine iliskin calismalar ve Kuzey Anadolu Fay problemi: Kuzey Anadolu Fayi ve Deprem Kusagi Simpozyumu. *MTA Yayinl., Ankara*, **12**, 35–58.

—— 1971. Focal mechanism and source depth of earthquakes from body- and surface-wave data. *Bull. Seism. Soc. Am.* **61**, 1369–79.

—— & EZEN, U. 1973. Slip rate and stress drop along the North Anatolian Fault. *In: Symposium*

on Earthquake Statistics. UNESCO Balkan Project, Istanbul.
—— & UCER, S. B. 1967a. Computer determinations for the fault-plane solutions in and near Anatolia. *Tectonophysics*, **4**, 235–44.
—— & —— 1967b. *A Catalogue of Focal Mechanism Diagrams for Turkey and Adjoining Areas. I.T.U. Maden Fak. Arz Fiziji Enst. Yay.* **25**, 111 pp.
CHEN, R. & MOLNAR, P. 1981. Constraints on seismic wave velocity structure beneath the Tibetan plateau and their tectonic implications, *J. geophys. Res.* **86**, 5937–62.
—— & —— 1983. Focal depths of intracontinental and intraplate earthquakes and their implication for the thermal and mechanical properties of the lithosphere. *J. geophys. Res.* **88**, 4183–214.
CHINNERY, M., 1969. Theoretical fault models. *In: A Symposium on Processes in Focal Region. Publ. Dem. Obs., Ottawa, Canada.* **7**, 211–23.
CONEY, P. J., JONES, D. L. & MONGER, J. W. 1980. Cordilleran suspect terranes. *Nature, Lond.* **288**, 329–33.
COOK, F. A., ALBAUGH, D. S., BROWN, L. D., KAUFMAN, S., OLIVER, J. E. & HATCHER, R. D. 1979. Thin-skinned tectonics in the crystalline southern Appalachians; COCORP seismic-reflection profiling of the Blue Ridge and Piedmont. *Geology*, **7**, 563–7.
CROWELL, J. A. 1974. Origin of late Cenozoic basins in southern California. *Spec. Publ. Soc. econ. Palaeont. Miner., Tulsa,* **22**, 190–240.
CUMMINGS, D. 1976. Theory of plasticity applied to faulting, Mojave Desert, southern California. *Bull. geol. Soc. Am.* **87**, 720–4.
DAS, S. & SCHOLZ, C. H. 1983. Why large earthquakes do not nucleate at shallow depths. *Nature, Lond.* **305**, 621–3.
DEGENS, E. T. & KURTMAN, F. 1978. The geology of Lake Van. *MTA Yaginl. Ankara,* **169**, 158 pp.
DELAUNE-MAYERE, M., MARCOUX, J., PARROT, J. F. & POISSON, A. 1977. Modele d'evolution Mesozoique de la paleo-marge tethysienne au niveau des nappes radiolaritiques et ophiolitiques du Taurus Lycien, d'Antalya et du Baer-Bassit: *In*: BIJU-DUVAL, B. & MONTADERT, L. (eds) *Structural History of the Mediterranean Basins*. pp. 79–94. Editions Technip, Paris.
DEWEY, J. F. 1969. Structure and sequence in the paratectonic Caledonides. *Amr. Ass. petrol. geol. Mem.* **12**. 309–35.
—— 1975. Finite plate evolution: some implications for the evolution of rock masses at plate margins. *Am. J. Sci.* **275-A**, 260–84.
—— 1977. Suture zone complexities: a review. *Tectonophysics*, **40**, 53–67.
—— 1980. Episodicity, sequence, and style at convergent plate boundaries. *Geol. Ass. Can. Spec. Pap.* **2**, 553–76.
—— 1982. Plate tectonics and the evolution of the British Isles. *J. geol. Soc. London,* **139**, 371–412.
—— & BURKE, K. C. A. 1973. Tibetan, Variscan and Precambrian basement reactivation: products of continental collision, *J. Geol.* **18**, 683–92.
—— & KIDD, W. S. F. 1974. Continental collisions in the Appalachian/Caledonian Orogenic Belt: variations related to complete and incomplete suturing. *Geology*, **2**, 543–6.
——, PITMAN III, W. C., RYAN, W. B. F. & BONNIN, J. 1973. Plate tectonics and the evolution of the Alpine System. *Bull. Geol. Soc. Am.* **84**, 3137–80.
—— & SENGOR, A. M. C. 1979. Aegean and surrounding regions: complex multi-plate and continuum tectonics in a convergent zone. *Bull. geol. Soc. Am.* **90**, 84–92.
—— & SHACKLETON, R. M. 1984. A model for the evolution of the Grampian Tract in the early Caledonides and Appalachians. *Nature, Lond.* **312**, 115–21.
—— & WINDLEY, B. F. 1981. Growth and differentiation of the continental crust. *Phil. Trans. R. Soc. London,* **A301**, 189–206.
DEWEY, J. W. 1976. Seismicity of northern Anatolia. *Bull. Seism. Soc. Am.*, **66**, 843–68.
DURR, S., ALTHERR, R., KELLER, J., OKRUSCH, M. & SEIDEL, E. 1978. The median Aegean crystalline belt: stratigraphy, structure, metamorphism, magmatism. *In*: CLOSS, H. (ed.) *Mediterranean Orogens*, pp. 48–72. E. Schweizerbart'sche Vertlagsbach-handlung, Stuttgart.
EATON, J. P., LEE, W. H. K. & PAKISER, L. C. 1970. Use of microearthquakes in the study of the mechanics of earthquake generation along the San Andreas Fault in Central California. *Tectonophysics*, **9**, 259–82.
ENGLAND, P. C. 1978. Some thermal considerations of the Alpine metamorphism — past, present and future. *Tectonophysics*, **46**, 21–40.
—— 1983. Constraints on the extension of continental lithosphere. *J. geophys. Res.* **88**, 1145–52.
—— & MCKENZIE, D. P. 1982. A thin viscous sheet model for continental deformation. *Geophys. J. R. astr. Soc.* **70**, 295–321.
ERGIN, K., GUSLU, U. & UZ, Z. 1967. A catalogue of earthquakes of Turkey and surrounding area (11 AD to 1964 AD). *Maden Fak. Arz Fizigi Enst. Yayinlari, Istanbul*, **24**, 1–28.
ERINC, S., 1973. Turkiyenin sekillenmesinde neotektonigin rolu ve jeomorfoloji-jeodinamik iliskileri. Cumburiyetin 50. Yili yerbilimleri Kongresi 1–12.
GANSSER, A. 1968. The Insubric Line, a major geotectonic problem. *Schweiz. Miner. Petrogr. Mitt.* **48**, 123–43.
—— 1974. The ophiolitic mélange, a world-wide problem on Tethyan examples. *Eclog. Geol. Helv.* **67**, 479–507.
GEISER, P. & ENGELDER, T. 1983. The distribution of large parallel shortening fabrics in the Appalachian foreland of New York and Pensylvania. *Mem. geol. Soc. Am.* **158**, 161–75.
HALL, R 1976. Ophiolite emplacement and the evolution of the Taurus Suture Zone, south-eastern Turkey. *Bull. geol. Soc. Am.* **87**, 1078–88.
HANCOCK, P. L. & BARKA, A. A. 1981. Opposed shear senses inferred from neotectonic meso-

fracture systems in the North Arabian Fault Zone. *J. struct. Geol.* **3**, 383–92.
——, Al Kadhi, A. & Sha'at, N.A. 1984. Regional joint sets in the Arabian Platform as indicators of intraplate processes. *Tectonics*, **3**, 27–43.
Hanks, T. C. & Wyss, M. 1972. The use of body-wave spectra in the determination of seismic-source parameters. *Bull. Seism. Soc. Am.* **62**, 561–89.
Hempton, M. R. 1980. Structure and morphology of the East Anatolian Transform Fault Zone near Lake Hazar. *GSA Annual Meeting Abs. with Programs*, **12**, 445.
—— 1982. The North Anatolian Fault and complexities of continental escape. *J. struct. Geol.* **4**, 502–4.
—— & Dewey, J. F. 1983. Earthquake-induced deformational structures in young lacustrine sediments, East Anatolian Fault, southeast Turkey. *Tectonophysics*, **98**, 7–14.
——, Dunne, L. A. & Dewey, J. F. 1983. Sedimentation in a modern strike-slip basin, southeastern Turkey. *J. Geol.* **91**, 401–12.
—— & Sengor, A. M. C. 1980. The East Anatolian transform fault: its age offset and significance in the neotectonics of the eastern Mediterranean. *EOS*, **61**, 360.
Houseman, G. A., McKenzie, D. P. & Molnar, P. 1981. Convective instability of a thickened boundary layer and its relevance for the thermal evolution of continental convergent belts. *J. geophys. Res.* **86**, 6115–35.
Hsü, K. J., Nachev, I. K. & Vuchev, V. T. 1977. Geologic evolution of Bulgaria in light of plate tectonics. *Tectonophysics*, **40**, 245–56.
Hutton, D. H. W. 1979. The strain history of a Dalradian slide using pebbles with low fluctuations in axis orientation. *Tectonophysics*, **55**, 261–73.
Innocenti, P., Mazzuoli, R., Pasquare, G., Radicati di Brozolo, F. & Villare, L. 1976. Evolution of the volcanism in the area of interaction between the Arabian, Anatolian and Iranian Plates (Lake Van, eastern Turkey). *J. Volcan. Geotherm. Res.* **1**, 103–12.
Jackson, J. A. 1980. Reactivation of basement faults and crustal shortening in orogenic belts. *Nature, Lond.* **283**, 343–6.
—— & McKenzie, D. P. 1983. Active tectonics of the Alpine-Himalayan Belt between western Turkey and Pakistan. *Geophys. J. R. astr. Soc.* **77**, 185–264.
Karner, G. D. & Watts, A. B. 1983. Gravity anomalies and flexure of the lithosphere at mountain ranges. *J. geophys. Res.* **88**, 449–60.
Ketin, I., 1948. Uber die tektonisch-mechanischen Folgerungen aus den grossen anatolischen Erdbeben des letzten Dezenniums. *Geol. Rdsch.* **36**, 77–83.
—— 1957. Kuzey Anadolu Deprem. Fayi. *ITU Dergisi*, **15**, 49–52.
—— 1966a. Tectonic units of Anatolia. *Bull. miner. Res. Explor. Inst. Ankara*, **66**, 23–34.
—— 1966b. 6 Ekim 1964 Manyas depremi espasinda zeminde meydana gelen tansiyon catlaklari. *Turkiye Jeoloji Kurumu Bulteni*, **10**, 1–2.
—— 1969. Ober die nordanatolische Horizontalverschiebung. *Bull. miner. Res. Explor. Inst. Ankara*, **72**, 1–28.
—— 1970. Bati Anadolu Neojen havzalarinin sismotektonik durumu. Gediz Depremi Zimopozyumu, Tebligler,Tanismalar, Insaat Muhendisleri Odasi, Ankara, pp. 8–16.
—— 1976. San Andreas ve Kuzey Anadolu Faylari arasinda bir karsilastirma. *Turkiye Jeoloji Kurumu Bulteni*, **19**, 149–54.
—— & Roasli, F. 1953. Maskroseismische Untersuchungen uber das nordwest-anatolische Beben vom 18. Marz 1953. *Eclog. Geol. Helv.* **46**, 187–208.
Kirby, S. H. 1980. Tectonic stresses in the lithosphere: constraints provided by the experimental deformation of rocks. *J. geophys. Res.* **85**, 6353–63.
Laubscher, H. P. 1971. Das Alpen-Dinariden Problem und die Palinspastik der sudichen Tethys. *Geol. Rdsch.* **60**, 813–33.
Luyendyk, B. P., Kamerling, M. J. & Terres, R. 1980. Geometrical model for Neogene crustal reactions in southern California. *Bull. geol. Soc. Am.* **91**, 211–8.
Lynn, H. B., Hale, L. D. & Thompson, G. A. 1981. Seismic reflections from the basal contacts of batholiths. *J. geophys. Res.* **86**, 10633–8.
Mattauer, M., Proust, F. & Tapponnier, P. 1972. Major strike-slip fault of late Hercynian age in Morocco. *Nature, Lond.* **237**, 160–2.
McKenzie, D. P. 1972. Active tectonics of Mediterranean region. *Geophys. Jl*, **18**, 1–32.
—— 1972. Active tectonics of the Mediterranean Region. *Geophys. J. R. astr. Soc.* **30**, 109–85.
—— 1976. The East Anatolian Fault: a major structure in eastern Turkey. *Earth planet. Sci. Lett.* **29**, 189–93.
—— & Jackson, J. A. 1983. The relationship between strain rates, crustal thickening, palaeomagnetism, finite strain and fault movements within a deforming zone. *Earth planet. Sci. Lett.* **65**, 182–202.
Meissner, R. & Strehlau, J. 1982. Limits of stresses in continental crust and their relationship to the depth-frequency of shallow earthquakes. *Tectonics*, **1**, 73–89.
Minster, J. B., Jordan, T. H., Molnar, P. & Haines, E. 1974. Numerical modelling of instantaneous plate tectonics. *Geophys. J. R. Astr. Soc.* **36**, 541–76.
Mohajer-Ashjai, A., Behzadi, H. & Berberian, M. 1975. Reflections on the rigidity of the Lut block and recent crustal deformation in eastern Iran. *Tectonophysics*, **25**, 281–301.
Molnar, P. & Chen, W. R. 1983. Focal depths and fault plane solutions of earthquakes under the Tibetan plateau. *J. Geophys. Res.* **88**, 1180–96.
—— & Tapponnier, P. 1975. Cenozoic tectonics of Asia: effects of a continental collision. *Science*, **189**, 419–26.
—— & —— 1977a. Relation of the tectonics of eastern China to the India–Eurasia collision: application of slip line field theory to large-scale

continental tectonics. *Geology*, **5**, 212–6.

____ & ____ 1977b. Active faulting and tectonics in China. *J. geophys. Res.* **82**, 2905–30.

____ & ____ 1978. Active tectonics of Tibet. *J. geophys. Res.* **83**, 5361–75.

____ & ____ 1979. Active faulting and Cenozoic tectonics of the Tien Shan, Mongolia and Bayka regions. *J. geophys. Res.* **84**, 3425–59.

____ & ____ 1981. A possible dependence of tectonic strength on the age of the crust in Asia. *Earth planet. Sci. Lett.* **52**, 107–14.

MTA 1962. *Explanatory Text of the Geological Map of Turkey, 1/500,000*, 75 pp. MTA Enstitusu, Ankara.

Ni, J. & Barazangi, M. 1984. Seismotectonics of the Himalayan collision zone: geometry of the underthrusting Indian Plate beneath the Himalayas. *J. geophys. Res.* **89**, 1147–63.

____ & York, J. E. 1978. Late Cenozoic tectonics of the Tibetan Plateau. *J. geophys. Res.* **83**, 5377–48.

Nowack, E. 1928. Die wichtigsten Ergebnisse meiner anatolischen Reisen. *Z dt geol.Ges.* **80**, B304–12.

Ozgul, N. 1976. Toroslar' in bazi temel jeoloji ozellikleri. *Tuirkiye Jeoloji Kurumu Bulteni*, **19**, 65–78.

Pamir, R. N. 1950. Les seismes en Asie Mineure entre 1939 et 1944. La Cicatrice Nord-Anatolienne. *Proc. Int. Géol. Congr. Lond.* **13**, 214–8.

____ & Akyol, I. H. 1943. Corum ve Erbaa depremieri. *Turk Cografya Dergisi*, **2**, 1–7.

____ & Ketin, I. 1940. Das Erbdeben in der Turkei vom 27 und 28 Dezember 1939. *Geol. Rdsch.* **31**, 77–8.

____ & ____ 1941. Das anatolische Erdbeben Ende 1939. *Geol. Rdsch.* **32**, 279–87.

Parejas, E., Akyol, I. H. & Altinii, E. 1942. Le tremblement de terre d'Erzincan due 27 Decembre 1939. *Revue Fac.Sci. Univ. Istanbul*, **BVI**, 177–222.

Pavoni, N. 1961a. Die Nordanatolische Horizontalverschiebung. *Geol. Rdsch.* **51**, 122–39.

____ 1961b. Faltung durch Horizontalverschiebung. *Eclog. geol. Helv.* **54**, 515–34.

Pfiffner, O. A. & Ramsay, J. G. 1982. Constraints on geological strain rates, arguments from finite strain states of naturally deformed rocks. *J. geophys. Res.* **87**, 311–21.

Powell, C. McA. & Conaghan, P. J. 1973. Plate tectonics and the Himalayas. *Earth planet. Sci. Lett.* **20**, 1–20.

Prescott, A. & Nur, A. 1981. The accommodation of relative motion at depth on the San Andreas Fault System in California. *J. geophys. Res.* **85**, 999–1004.

Ramsay, J. G. & Wood, D. S. 1976. A discussion on natural strain and geological structure. *Phil. Trans. R. Soc. London*, **A283**, 344 pp.

Ricou, L. E., Argyriadis, I. & Marcoux, J. 1975. L'Axe Calcaire du Taurus, un alignment de fenetres araboafricaines sous des nappes radiolaritiques, ophiolitiques et metamorphignes. *Bull. Soc. geol. France* **17**, 1024–44.

Roeder, D. 1979. Continental collisions. *Rev. Geophys. Space Phys.* **17**, 1098–109.

von Rogl, F. & Steininger, F. F. 1983. Vom Zerfall der Tethys zu Mediterran und Paratethys. *Ann. Naturhist. Mus. Wien,* **85/A**, 135–63.

Royden, L., Horvath, F. & Rumpler, J. 1983. Evolution of the Pannonian Basin System. I. Tectonics. *Tectonics*, **2**, 63–90.

Rybach, L., Mueller, S., Milnes, A. G., Ansorge, J., Bernoulli, D. & Frey, M. 1980. The Swiss Geotraverse Basel-Chiasser — a review *Eclog. Geol. Helv.* **73**, 437–62.

Salomon-Calvi, W. 1936a. Die Fortsetzung der Tonalelinie in Kleinasien. *Yuksek Ziraat Enst. Calismalarindan*, **9**, 11–3.

____ 1936b. Die Entstehung der anatolischen Ova. *Yuksek Ziraat Enst. Calismalarindan*, **30**, 11 pp.

____ 1940. Anadolu'num tektonik tarzi tesekkulu hakklinda kisa izahat. *MTA Mecmuasi*, **18**, 35–47.

Scholz, C. H. 1977. Transform fault systems of California and New Zealand: similarities in their tectonic and seismic styles. *J. geol. Soc. London*, **133**, 215–29.

Sclater, J. G. & Francheteau, J. 1970. The implications of terrestrial heat flow observations on current tectonic and geochemical models of the crust and upper mantle of the earth. *Geophys. J.R. astr. Soc.* **20**, 509–42.

Sengor, A. M. C., 1976. Collision of irregular continental margins: implications for foreland deformation of Alpine-type orogens. *Geology*, **4**, 779–82.

____ 1977. Post-Miocene tectonic evolution of eastern Turkey: initial stages in the formation of a Tibetan-type high plateau. *Geol. Soc. Am., Abst. Prog.* **9**, 1168–76.

____ 1979. North Anatolian Fault: its age offset and tectonic significance. *J. geol. Soc. London*, **136**, 269–82.

____ & Kidd, W. S. F. 1979. Post-collisional tectonics of the Turkish–Iranian plateau and a comparison with Tibet. *Tectonophysics*, **55**, 361–76.

Seymen, I. 1975. *Kelkit vadisie kesiminde Kuzey Anadolu Fay Aonunun tektonik ozelligi*, 192 pp. ITU Maden Fak Yay, Istanbul.

____ & Aydin, A. 1972. The Bingol Earthquake Fault and its relation to the North Anatolian Fault Zone. *Bull. miner. Res. Explor. Inst. Ankara*, **79**, 1–8.

Sibson, R. H. 1983. Continental fault structure and the shallow earthquake source. *J. geol. Soc. London*, **140**, 741–67.

Sieh, K. E. 1978. Prehistoric large earthquakes produced by slip on the San Andreas Fault at Pallet Creek, California. *J. geophys. Res.* **83**, 3907–39.

Sims, J. D. 1973. Earthquake-induced structures in sediments of Van Norman Lake, San Fernando, California. *Science*, **182**, 161–3.

____ 1975. Determining earthquake recurrence intervals from deformational structures in young lacustrine sediments. *Tectonophysics*, **29**, 141–52.

Swan III, F. H., Schwartz, D. P. & Cluff, L. S.

1980. Recurrence of moderate to large magnitude earthquakes produced by surface faulting on the Wasatch Fault Zone, Utah. *Bull. seismol. Soc. Am.* **70**, 1431–62.

TAPPONNIER, P. 1977. Evolution tectonique du Systeme Alpin en Medtierranée: poinconnement et ecrasement rigide-plastique. *Bull. Soc. géol. France*, **19**, 437–60.

—— & MOLNAR, P. 1976. Slip-line field theory and large-scale continental tectonics. *Nature, Lond.* **264**, 319–21.

—— & —— 1977. Active faulting and tectonics in China. *J. geophys. Res.* **82**, 2905–30.

——, MERCIER, J. L. ARMIJO, R. HAN TONGLIN & ZHOU, J. 1981. Field evidence for active normal faulting in Tibet. *Nature, Lond.* **294**, 410–4.

——, PELTZER, G., LE DAIN, A. Y., ARMIJO, R. & COBBOLD, P. 1982. Propagating extrusion tectonics in Asia: new insights from simple experiments with plasticene. *Geology*, **10**, 611–6.

TATAR, Y. 1975. Tectonic structures along the North Anatolian Fault Zone, north-east of Refahiye (Erzincan). *Tectonophysics*, **29**, 401–10.

TCHALENKO, J. S. 1977. A reconnaissance of the seismicity and tectonics at the northern border of the Arabian Plate (Lake Van Region). *Rev. Geogr. Phys. Geol. Dyn.* **19**, 189–208.

TOKAY, M. 1973. Kuzey Anadolu Fay Zonunun Gerede ile Ilgaz arasindaki kisminda jeolojik gozlemler. *Kuzey Anadoluy Fayi ve Deprem Kusagi Simpozyumu*, pp. 12–29. MTA Yayini, Ankara.

TOKSOZ, M. N., ARPAT, E. & SAROGLU, F. 1977. East Anatolian earthquake of 24 November 1976. *Nature, Lond.* **270**, 423–5.

TRUMPY, R. 1973. The timing of orogenic events in the Central Alps. *In:* DEJONG, K. A. & SCHOLTEN, R. (eds) *Gravity and Tectonics*, pp. 229–251. John Wiley and Sons, New York.

UGUR, E. 1974. Recent crustal movements in the Gerede-Cerkes region of the North Anatolian Fault Zone by Geodetic Methods. Ph.D. thesis, I.T.U., Istanbul.

WALLACE, R. E. 1968. Earthquake of August 19, 1966, Varto area, eastern Turkey. *Bull. Seism Soc. Am.* **58**, 11–45.

—— 1977. Time-history analysis of fault scarps and fault traces — a longer view of seismicity. *In: Proceedings of the 6th World Conference on Earthquake Engineering, New Delhi, India,* **1**, 766–9.

—— 1978. Patterns of faulting and seismic gaps in the Great Basin province. *In: Proceedings of Conference VI, Methodology for Identifying Seismic Gaps and Soon-to-break Gaps. U.S. geol. Survey Open File Rep.* **78–943**, 858–68.

YODER, H. S. & TILLEY, C. E. 1962. Origin of basalt magmas: an experimental study of natural and synthetic rock systems. *J. Petrol.* **3**, 342–532.

J. F. DEWEY, Department of Earth Sciences, University of Oxford, Oxford OX1 3PR, UK.

M. R. HEMPTON, Bellaire Research Center, Shell Development Company, Houston, Texas, U.S.A.

W. S. F. KIDD, Department of Geological Sciences, State University of New York, Albany, New York, U.S.A.

F. SAROGLU, Maden Tetkik ve Arama, Ankara, Turkey.

A. M. C. ŞENGÖR, Faculty of Geology, Istanbul Technical University, Istanbul, Turkey.